การตรวจหาสิ่งพกพาด้วยโครงร่างรูปดาวแบบเซนทรอยด์ปรับตัว

นางสาววรินท์ ชยานุรักษ์

วิทยานิพนธ์นี้เป็นส่วนหนึ่งของการศึกษาตามหลักสูตรปริญญาวิทยาศาสตรมหาบัณฑิต
สาขาวิชาวิทยาการคอมพิวเตอร์และเทคโนโลยีสารสนเทศ
ภาควิชาคณิตศาสตร์และวิทยาการคอมพิวเตอร์
คณะวิทยาศาสตร์ จุฬาลงกรณ์มหาวิทยาลัย
ปีการศึกษา 2554

ลิขสิทธิ์ของจุฬาลงกรณ์มหาวิทยาลัย
บทคัดย่อและแฟ้มข้อมูลฉบับเต็มของวิทยานิพนธ์ตั้งแต่ปีการศึกษา 2554 ที่ให้บริการในคลังปัญญาจุฬาฯ (CUIR)
เป็นแฟ้มข้อมูลของนิสิตเจ้าของวิทยานิพนธ์ที่ส่งผ่านทางบัณฑิตวิทยาลัย
The abstract and full text of theses from the academic year 2011 in Chulalongkorn University Intellectual Repository(CUIR)
are the thesis authors' files submitted through the Graduate School.

CARRYING OBJECT DETECTION USING ADAPTIVE CENTROID STAR SKELETON

Miss Rawin Chayanurak

A Thesis Submitted in Partial Fulfillment of the Requirements

for the Degree of Master of Science Program in Computer Science and Information Technology

Department of Mathematic and Computer Science

Faculty of Science

Chulalongkorn University

Academic Year 2011

Copyright of Chulalongkorn University

Thesis Title	CARRYING OBJECT DETECTION USING ADAPTIVE CENTROID STAR SKELETON
By	Miss Rawin Chayanurak
Field of Study	Computer Science and Information Technology
Thesis Advisor	Assistant Professor Nagul Cooharojananone, Ph.D.

Accepted by the Faculty of Science, Chulalongkorn University in Partial Fulfillment of the Requirements for the Master's Degree

..... Dean of the Faculty of Science
(Professor Supot Hannongbua, Ph.D.)

THESIS COMMITTEE

..... Chairman
(Assistant Professor Rajalida Lipikorn, Ph.D.)

..... Thesis Advisor
(Assistant Professor Nagul Cooharojananone, Ph.D.)

..... External Examiner
(Rawesak Tanawongsuwan, Ph.D.)

รวินท์ ชยานุรักษ์: การตรวจหาสิ่งพกพาด้วยโครงร่างรูปดาวแบบเซนทรอยด์ปรับตัว. (CARRYING OBJECT DETECTION USING ADAPTIVE CENTROID STAR SKELETON) อ. ที่ปรึกษาวิทยานิพนธ์หลัก : ผศ. ดร. นกุล คูหะโรจนานนท์, 75 หน้า.

การตรวจหาสิ่งพกพาเป็นหนึ่งในขั้นแรกของโปรแกรมการตรวจตารักษาความปลอดภัยซึ่งมีประโยชน์ในการเฝ้าดูและตรวจตราการคุกคามและยังป้องกันอาชญากรรมเพื่อดำรงการควบคุมทางสังคม ดังนั้นวิทยานิพนธ์ฉบับนี้ได้มีเป้าหมายเพื่อตรวจหาสิ่งพกพาที่มองจากกล้องวิดีโอซึ่งอยู่นิ่งโดยใช้ข้อมูลเงาของคนในการค้นหา เทคนิคโครงร่างรูปดาวแบบเซนทรอยด์ปรับตัวได้ถูกนำมาใช้เพื่อให้ได้มาซึ่งลักษณะของคน สิ่งพกพาจะถูกแยกแยะโดยใช้อนุกรมเวลาของการเคลื่อนไหวของกิ่งของโครงสร้างรูปดาว กรอบของสิ่งพกพาคำนวนได้จากจุดที่พบสิ่งพกพากับจุดใกล้เคียงในกราฟของการคำนวนโครงสร้างรูปดาว วิธีการนี้สามารถตรวจจับและติดตามสิ่งพกพาเช่นกระเป๋าสะพายและกระเป๋าลาก มากกว่านั้นยังสามารถตรวจหาเหตุการณ์ที่กระเป๋าลากถูกทิ้งได้ ในการวิจัยนี้ได้นำข้อมูลจากTRECVIDและวิดีโอถ่ายเองมาใช้ในการทดสอบ

ภาควิชา คณิตศาสตร์และวิทยาการคอมพิวเตอร์ ลายมือชื่อนิสิต .....

สาขา วิชา วิทยาการ คอมพิวเตอร์ และ เทคโนโลยี สารสนเทศ ..... ลายมือชื่อ อ.ที่ปรึกษาวิทยานิพนธ์หลัก .....

ปีการศึกษา ..... 2554 .....

5273611023: MAJOR COMPUTER SCIENCE AND INFORMATION TECHNOLOGY
KEYWORDS: CARRIED OBJECT / STAR SKELETON / ADAPTIVE CENTROID

RAWIN CHAYANURAK : CARRYING OBJECT DETECTION USING ADAPTIVE CENTROID STAR SKELETON. ADVISOR : ASST. PROF. NAGUL COOHAROJANANONE, Ph.D., 75 pp.

Detecting a carried object is a primary step for surveillance applications which is useful to recognize and monitor threats, and prevent criminal activity in order to maintain social control. Thus, this thesis aims to detect a carried object seen from a stationary camera using human body silhouette feature information. Star skeletonization technique with the adaptive centroid point is used to extract human feature. The carried object is classified using time series of motions of the extracted skeleton limbs. The boundary of the carried object is figured from carried objects track points and adjacent sink curves of contour. The method is able to detect and track carried object such as a luggage and a backpack. Moreover, the detection of leaving luggage event could be achieved. In the research, some data from TRECVID dataset and manually captured data are used to perform experiments.

Department : Mathematic and Computer Science
Field of Study : Computer Science and Information Technology . . . . . .
Academic Year . . . . . 2011 . . . . . .

Student's Signature . . . . . .
Advisor's Signature . . . . . .

Acknowledgements

I would like to thank all people who have helped and inspired me during my study. I deeply indebted to my advisor, Assistant Professor Nagul Cooharojananone, for his guidance during my research and study. Deepest gratitude are also due to the members of the thesis committee, Assistant Professor Rajalida Lipikorn and Dr. Rawesak Tanawongsuwan who spent their precious times for giving invaluable opinions. I also wishes to express my love and gratitude to my beloved families. Without their encouragement and support I could not be able to carry out this thesis, especially my mother who always understand and cheer me. Special thanks also to my friends, especially Siriwat Kasamwattanarote for sharing the literature and helpful assistance. There are more people that I would like to thank. Their names may not be written here, but they are, everlastingly, written in my heart.

Contents

Page

Abstract (Thai) . . . iv

Abstract (English) . . . v

Acknowledgements . . . vi

Contents . . . vii

List of Tables . . . ix

List of Figures . . . x

Chapter

I INTRODUCTION . . . **1**

1.1 Motivation and Problem Description . . . 1

1.2 The Objective of Research . . . 1

1.3 The Scope of Study . . . 1

1.4 Expected Outcomes . . . 2

1.5 The Benefits of Research . . . 2

II RELATED WORKS, PRINCIPLES OF EXPERIMENT . . . **3**

2.1 Related Works . . . 3

2.2 Principles of experiment . . . 5

2.3 Star Skeleton . . . 6

2.4 Delaunay Triangulation . . . 7

2.4.1 Constrained Delaunay Triangulation . . . 9

III EXPERIMENTAL DESIGN AND METHODLOGY . . . **10**

3.1 Preprocessing . . . 10

3.2 Calculating Centroid . . . 10

3.3 Star Skeletonization . . . 15

3.4 Tracking . . . 15

3.5 Normalizing the Tracked Position . . . 16

3.6 Carried Object detection . . . 16

3.6.1 Time series . . . 19

3.6.2 Mean difference and Standard deviation . . . 19

3.6.3 Area of consideration . . . 20

Chapter Page

3.6.4 Motion History Image 21
3.7 Carried Object Boundary Approximation 23

IV EXPERIMENTAL RESULTS 24
4.1 Results from manually foreground extracted sequences 24
4.2 Results from automatically foreground extracted sequences 26
4.3 Improvement by Standard deviation, Area of consideration and Motion History image 30
4.4 Weight Parameter 36
4.5 Threshold Parameter 36
4.6 Video captured in other view point 37

V CONCLUSIONS AND FUTURE WORKS 39
5.1 Conclusion 39
5.2 Future Works 39
Appendix 43
Appendix A Results 43
Biography 64

List of Tables

Table Page

4.1 Samples of correctly detection of carried object. 27

4.2 Confusion matrix for carried object detection 30

List of Figures

Figure Page

2.1 Body main axis . . . 3
2.2 Non-symmetric region segmentation . . . 4
2.3 Eight exemplar temporal templates . . . 5
2.4 Demonstration of thinking for principles of experiment . . . 6
2.5 Distance signal . . . 6
2.6 Difference graph . . . 7
2.7 Delaunay triangulation . . . 8
2.8 PSLG graph and corresponding CDT . . . 8
2.9 Weaker Delaunay property . . . 8
3.1 Flow of methodology . . . 11
3.2 Video segment and resolved silhouette . . . 11
3.3 Silhouette and result contour . . . 12
3.4 Opened contour image and closed contour image . . . 12
3.5 Sample of star skeleton of backpack case . . . 12
3.6 Sample of star skeleton of luggage case . . . 13
3.7 Sample of finding control points for delaunay triangulation . . . 13
3.8 All the vertices for delaunay triangulation . . . 15
3.9 Process of star skeletonization . . . 15
3.10 Demonstration of the difference of size due to the difference dimension . . . 16
3.11 Sample of time series graph of tracked position and Time series graph of normalized tracked position . . . 17
3.12 Sample of time series graph of x value and y value of tracked objects . . . 17
3.13 Sample of Limb points of triangle-based skeleton that vary in a wide range from each frame . . . 18
3.14 Mean difference and standard deviation . . . 19
3.15 Failure of detecting shoulder and leg as carried objects . . . 20
3.16 Area of consideration around left and right . . . 21
3.17 Failure of miss carried object detection due to the high movement of x and y in time series graph . . . 21

Figure Page

3.18 Motion history image indicates area which is indifference with previous frames 22
3.19 Sample of distance graph of star skeleton represent peak points with adjacent sink curves to the carried object point 23
3.20 Another sample of distance graph of star skeleton represent peak points with adjacent sink curves to the carried object point 23
4.1 Samples of TRECVID dataset and manually captured data 24
4.2 Detection of luggage during the leaving luggage event 25
4.3 Results of sample video sequences. 26
4.4 Sample video sequence with true positive result 31
4.5 Sample video sequence with true negative result 31
4.6 Sample video sequence with false positive result 32
4.7 Sample video sequence with false negative result 32
4.8 Sample video sequence that could be improved by standard deviation 33
4.9 Sample video sequence that could be improved by Area of consideration and Motion History image 34
4.10 Steps of using Motion History image 34
4.11 Percentage of results 35
4.12 Accuracy of results with different weight compared 36
4.13 Accuracy of results with different threshold compared 37
4.14 Sample silhouette of sequences captured in other view point 38

CHAPTER I

INTRODUCTION

1.1 Motivation and Problem Description

Nowadays, surveillance camera is widely used because of the increasing of crime, terrorism and theft. However monitoring and inspecting events manually in daily surveillance video are the exhaustive tasks for human whose accuracy of work reduces by time. Surveillance applications have been developed to automate and ease those tasks and sometimes are able to replace human monitoring of some events. Detecting a carried object is a primary step for surveillance applications like detection of suspicious events such as left-luggage event, bag-prohibited area incursion.

1.2 The Objective of Research

This thesis purposes to study methodologies and techniques for develop a new method or improve existing method to detect a carried object moving along with walking people which is an initial step for some surveillance applications. With the first step achievement, next is to identify whether the detected carried object is left or not.

1.3 The Scope of Study

Scope of work can be described as follows:

1. Only image sequences of people walking straightly with carried objects not being completely occluded are used.
2. Only weighty carried objects such as luggage and backpack are focused.
3. Video is captured from a single stationary camera.

Therefore, any weighty carried object with walking people such as a luggage and a backpack is able to be detected as the limb track with motionless or which is only moving with the overall human body.

1.4 Expected Outcomes

The expected outcomes will be as follows:

1. A novel methodology to detect carried object with walking people in a video sequence.
2. An accurate technique to determine the left luggage event in a video sequence.

1.5 The Benefits of Research

The benefits of this research would be to provide the explanation of human posture using skeleton image representation. Techniques in this research would be able to be used to explore more explanations of human posture. Therefore, the algorithm would be widely used in by related organizations.

This thesis proposes a new method to detect a carried object with walking people in a video sequence. Chapter II provides related works and the details of related theory. Chapter III discusses the methodology testing of this study. The experiment results will be demonstrated in Chapter IV Chapter V points to conclusion and future works.

CHAPTER II

RELATED WORKS, PRINCIPLES OF EXPERIMENT

2.1 Related Works

There have been several attempts in this area. In paper (Qi et al., 2007; Haritaoglu et al., 1999), silhouette and main body axis are used to determine if a person is carrying an object. In (Qi et al., 2007), the carried object region can be found by accounting human contour shape by extracting the features from body main axis as in Figure 2.1, then finding the outmost point in human contour.

According to this method, body main axis could be found by the following equation 2.1

$$x_m = \frac{1}{k} \sum_{i=1}^{k} x_i \tag{2.1}$$

where x_i is the point on x axis and k is the number of points on the edge. If H is defined as standard height and H' is the original height, point on silhouette $P(x, y)$ can be normalized to $P'(x', y')$ according to the following equation.

$$\begin{cases} x' = x \\ y' = y \cdot \left(\frac{H'}{H}\right) \end{cases} \tag{2.2}$$

(a) (b)

Figure 2.1: (a) Body main axis and (b) features extracted from body main axis

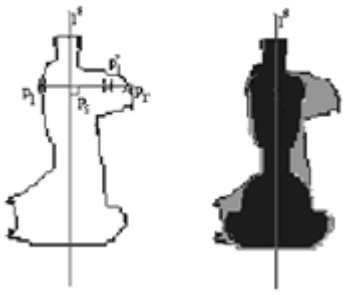

Figure 2.2: Non-symmetric region segmentation

As the assumption that the point on bag boundary is farthest from the body main axis compared to other points on the silhouette boundary. So, the distances from contour to the body main axis are defined as features. Finding the outmost point in human contour could be able to track a bag. Let the outmost vertex $P(x_p, y_p)$ be calculated as following equation

$$\begin{cases} x_p = \operatorname{Arg\,max} \|x_m - x\| \\ C\left(x_p, y_p\right) = 0 \end{cases} \tag{2.3}$$

Then bag region could be inferred from two points, $P_1(x_m - D, y_p)$ and $P_2(x_m, y_p + D)$ where D is the distance from P to body axis. A bag boundary rectangle is defined by these two points. In (Haritaoglu et al., 1999), the carried object is extracted from a person by silhouette analysis such as non-symmetric region extraction as in Figure 2.2. Silhouettes of human are typically close to symmetric about the body axis while standing, walking or running. Each pixel can be classified as symmetric or nonsymmetric as if its length to the body axis l^s is less than minimum of length from line l^s to each boundary on left and right side plus constant, this pixel is symmestric otherwise is nonsymmetric. Another approach is (DeCann and Ross, 2010), where gait curves are transformed into a one dimensional signal to determine the distortion of silhouette at back region due to presence of backpack. In (BenAbdelkader and Davis, 2002), Time series of bounding box width of human silhouettes are used to detect people carrying object. In (Vanacloig and Juan Alfonso Rosell Ortega, 2008), a classification method based on k-nearest neighbor classifiers and a voting system using two sets of features: foreground density features and features related to real-size of objects is introduced. The foreground density features are produced by dividing each tracked object into the same number of regions and calculating the proportion of foreground pixels to the total number of pixels for each of these regions. In (su Lee and Elgammal, 2006), pose preserving dynamic shape models are used to detect people carrying objects in

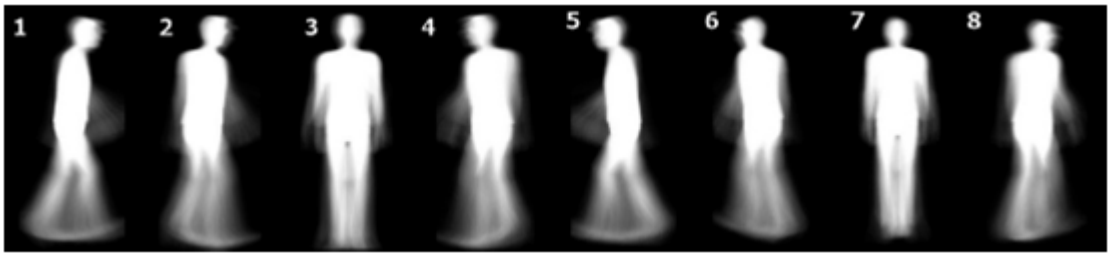

Figure 2.3: The eight exemplar temporal templates, created to represent 8 viewpoints

video sequences by means of their silhouette. Moreover, an iterative procedure of hole filling and outliers detection using pose preserving shape reconstruction is used to enhance the precision in the detection of people carrying objects. In (Senst et al., 2010) A periodicity dependency pattern describing the motion of a tracked person by using gray-value information instead of the contours obtained by a segmentation process is introduced. The intent is independent from the results of a background subtraction approach. People carrying objects are then classified using an off-line trained support vector machine. In (Damen and Hogg, 2008), the produce a representation of motion and shape (known as a temporal template) that has some immunity to noise in foreground segmentations and phase of the walking cycle. The temporal templates are matched with exempler templates generated with 3D Maya model in 8 view points as in Figure 2.3. The area that exceeds the best matched template is concerned. In (Chuang et al., 2009), the trajectory is used to get a ratio histogram for analyzing the relationship between the carried object and its owner. The carried object then can be found in the missing colors between ration histogram of a person with and without carried object. Then carried objects are segmented using Gaussian mixture models. Event analyzer using finite state machine is proposed to detect suspicious event.

2.2 Principles of experiment

After studying some of related works, some principles are realized for carried object detection. First of all is the principle of how to represent the human information which originally in video sequences into the form that can be interpreted. After that is to interpret those representations which the principle of how to translate the represented information into the expected meanings is next issue to think about as demonstrated in Figure 2.4. Studying several algorithms for action recognition resolves that star skeleton is one of the most popular representation techniques to represent human silhouette. In paper (Yu and Aggarwal, 2006; Chen et al., 2006; Petkovic et al., 2001; Putpuek et al., 2007), human features are represented by star skeleton. It is interesting to use star skeletonization to extract human feature in order to later translate its

Figure 2.4: Demonstration of thinking for principles of experiment

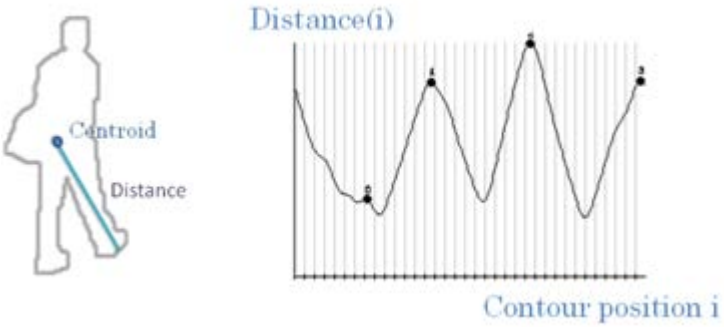

Figure 2.5: Distance signal (right) is constructed from distances from centroid to each contour point (left).

meanings.

2.3 Star Skeleton

The star skeleton means a star shaped skeleton which constructed from connecting lines from centroid to all extremities of a human boundary. The first step is to calculate the centroid of the target image boundary (x_c, y_c) (Chen et al., 2006)

$$\begin{aligned} \mathrm{x_c} &= \tfrac{1}{N_b} \textstyle\sum_{i=1}^{N_b} x_i \\ y_c &= \tfrac{1}{N_b} \textstyle\sum_{i=1}^{N_b} y_i \end{aligned} \tag{2.4}$$

where N_b is the number of border pixels, and (x_c, y_c) is a pixel on the contour of the target. Then find distance from the centroid (x_c, y_c) to each border point (x_i, y_i) using Euclidian Distance. The distances can be computed in a clockwise or counter-clockwise fashion. Then the distance signal in Figure 2.5 is smoothed by applying smoothing filter to reduce noise.

After that, local maximum or peak points are calculated by finding zero-crossings of the smoothed difference function. Zero-crossing means a point where the sign of a function changes from positive to negative as in Figure 2.6, represented by a crossing of the axis, zero value, in the graph of the function. Finally, the star skeleton is generated by joining these points to the centroid.

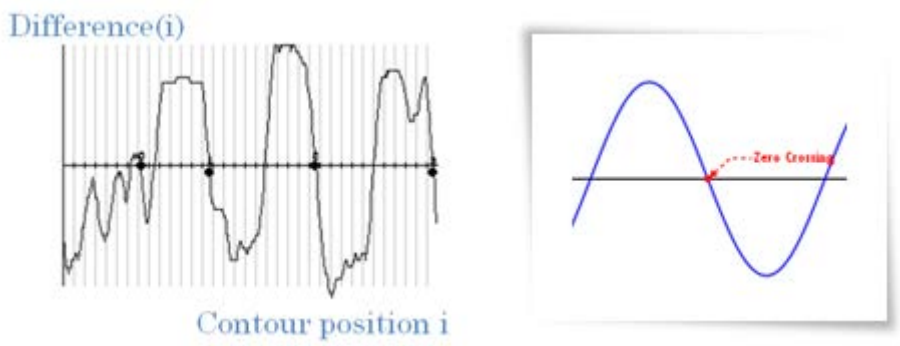

(a) (b)

Figure 2.6: (a)Difference graph of distance signal is analyzed to find limbs of skeleton by finding the (b) zero-crossing where the value crosses zero value.

In (Yu and Aggarwal, 2006), the centroid of a skeleton is moved from center to head to detect climbing fence event. In (Putpuek et al., 2007), the joints are added to a skeleton in order to represent silhouette of human in complex action like boxing. Realizing that centroid is moved from the original method for specific or complex action forces exploration for some methods to achieve this. Constrained Delaunay triangulation is used in (Chuang et al., 2008) to analyzed human posture and translate into star skeleton. From this paper, it is noticed that when constrained Delaunay triangulation is constructed from a human silhouette, the triangular mesh explore the shape of silhouette. Therefore, the constructed star skeleton has centroid that is at the joint of the body and arms or legs, which is interesting to use this technique for other posture.

2.4 Delaunay Triangulation

A Delaunay triangulation could be calculated from a set of points with some property. A triangulation whose all triangles have no point falls inside of their circumcircle, circle that passes through all three points of an triangle, as in Figure 2.7.

Delaunay triangles are said to be ”well shaped” because, in fulfilling the empty circumcircle property, triangles with larger internal angles are selected over the small internal angles. Also, the Delaunay triangulation connects points in a nearest-neighbor manner. These two characteristics, well-shaped triangles and the nearest-neighbor relation have important implications in practice and motivate the use of Delaunay triangulations in scattered data interpolation.

Figure 2.7: A Delaunay triangulation in the plane with circumcircles

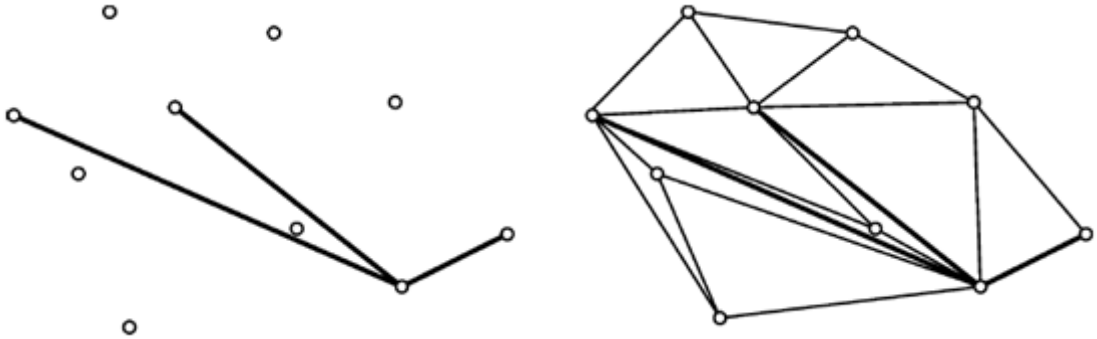

(a) (b)

Figure 2.8: (a)Input PSLG graph and (b) corresponding CDT

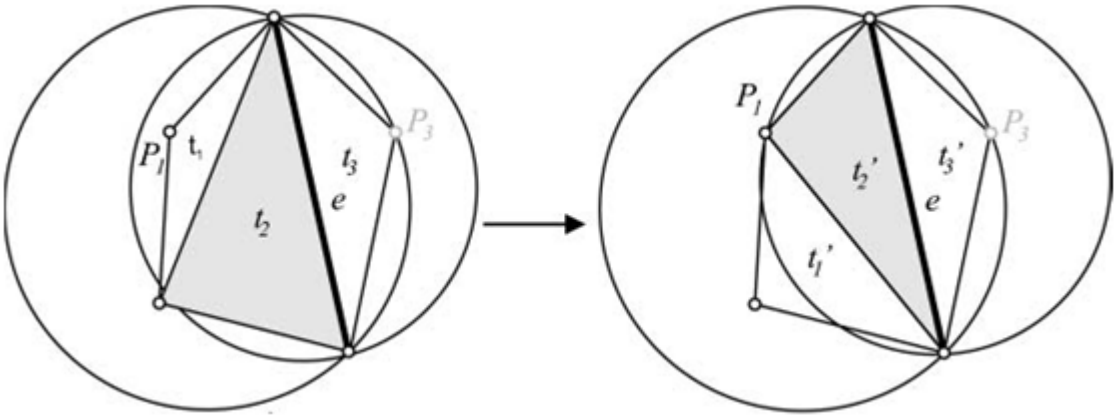

Figure 2.9: Weaker Delaunay property

2.4.1 Constrained Delaunay Triangulation

The constrained Delaunay triangulation is an extension of the Delaunay triangulation to handle constraints. Constrained triangulations are generally used to triangulate a nonconvex polygon. Constrained Delaunay triangulation is a generalized form of Delaunay triangulation, where the input is a planar straight-line graph, a graph with edges and straight lines without crossings in which every edges, described as $G = (V, E)$, where V is input points and E is input edges as Figure 2.8. From a property that the constraining edges should be edges of generated triangle, a weaker Delaunay property is used. In Figure 2.9(a), the circumcircle of triangle t_2 holds vertices P_1 and P_3, which violates Delaunay property. Then triangles t_1 and t_2 exchange their common edge to become the new triangles t_1 and t_2 as in Figure 2.9(b). This process is called legalization which is a recursive procedure. P_3 is not seen by t_2 as it is behind constraining edges e. Therefore, during legalizing t_2, P_3 is not involved. Constrained Delaunay triangulation discourages the property of validity of visible vertices. The definition of Delaunay triangulation and constrained Delaunay triangulation are the same except that, for the constrained Delaunay triangulation, portions of a circle are ignored whenever the circle passes through an edge.

There are several existing approaches to translate or classify motions as described in (Babu and Ramakrishnan, 2004), state-space based and template matching based approaches. State-space based approach uses time-series features obtained from image sequences are used for recognition. Template matching based approach uses the flow of information as feature. The temporal information in form of Motion History Image(MHi) obtained from accumulating sequences of motion images into a plane image is used for characterizing human actions. Thus, this thesis proposes carrying object detection using star skeleton representation of human features and adaptive centroid.

CHAPTER III

EXPERIMENTAL DESIGN AND METHODLOGY

To determine whether a walking person in a video sequence carries carried objects or not, human feature is extracted using star skeletonization with adaptive centroid and carried objects are determined from time series graph of limbs' positions from star skeleton. During each frame of video a star skeleton of the human silhouette is calculated. Then each limb's position of star skeleton is accumulated with of other frames' to measure the dispersion. The limb with low dispersion is resolved as carried object. Finally, the detected carried object's boundary is figured and the next frame is processed through the same algorithm until there is no frame further. The flow of methodology is as shown in Figure 3.1.

3.1 Preprocessing

With a sequence of human walking, next is to segment the foreground and to extract the contour of human. After foreground segmentation as in Figure 3.2, contour is extracted with canny edges (Canny, 1986) techniques, a detectors for arbitrary edges as Figure 3.3. Then an adjustment is done in order to get the correct sequence of contour points. The adjustment is needed to close the opened contour shape image as shown in Figure 3.4, which is done by smoothing the silhouette image before extraction of contour image and morphological filtering; dilating then erosion, after obtaining the contour image. A correct sequence of contour points can be obtained from adaptive contour image and ready to be used in the next step.

3.2 Calculating Centroid

In the star skeletonization process, the centroid plays an important role as a reference point to compute distances of contour points in order to find the skeleton. The original centroid point which is determined from averaging all contour points (Chen et al., 2006), sometimes misses some human features such as a carried object as shown in Figure 3.5.

The proposed method uses a centroid point obtained from the triangle-based skeleton which is extracted from the spanning tree generated from Delaunay triangle mesh of human shape. After those pre-processing steps, next is to generate triangular meshes on human silhouette using the constrained Delaunay triangulation technique. With a posture extracted in binary form by image

Figure 3.1: Flow of methodology

(a) (b)

Figure 3.2: (a) Video segment and(b) resolved silhouette

(a) (b)

Figure 3.3: (a) Silhouette and (b) result contour

(a) (b)

Figure 3.4: (a) Opened contour image and (b) closed contour image

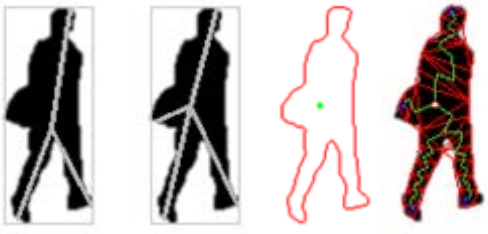

(a) (b) (c) (d)

Figure 3.5: (a) Sample of star skeleton generated with centroid from averaging of contours and (b) proposed star skeleton generated with (c) adaptive centroid from (d) a triangle-based skeleton's centroid in body region.

(a) (b) (c)

Figure 3.6: (a) Another sample of proposed star skeleton with (b) adaptive centroid from averaging (c) triangle-based skeleton's centroids in body region

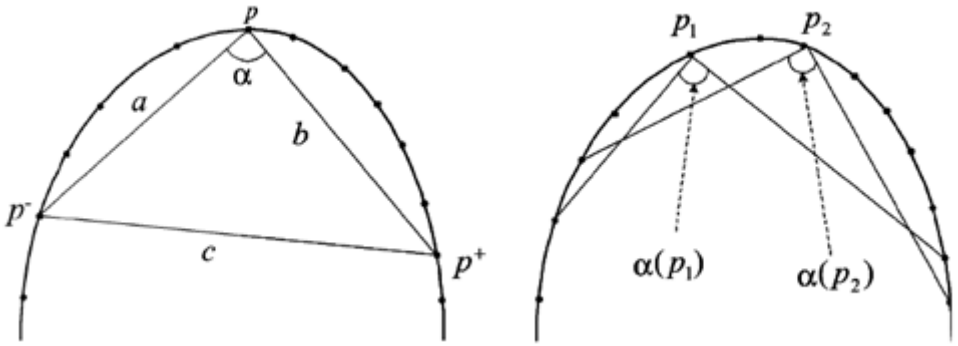

(a) (b)

Figure 3.7: Finding control points. (a) A point with a high curvature. (b) Two points with high curvatures that are too close to each other.

subtraction, and a set of control points extracted along its contour, a sample method to sample points along the contour as control points is done before generating Delaunay triangle mesh. As using all points along the silhouette's contour is not efficient. Sampling is needed to reduce points and follow (Chuang et al., 2008).

Assume that P is a feature silhouette from foreground subtraction. A set of control points extracted along its contour is used to triangulate P. Then some high curvature points as the set of control points from B ,the set of boundary points along the contour of P, are extracted. Let $\alpha(p)$ be the angle between a point p in B. As in Figure 3.7(a), two specified points is used to defined the angle $\alpha(p)$, p^+ and p^- can be selected from both sides of p along B.

$$\begin{aligned} d_{\min} \leq |p - p^+| \leq d_{\max} \\ d_{\min} \leq |p - p^-| \leq d_{\max} \end{aligned} \tag{3.1}$$

The equation 3.1 shows d_{min} and d_{max} which are two thresholds set to $|B|/30$ and, $|B|/20$ respectively. $|B|$ is the total length of contour of B. Thus the angle can be determined by equation /refeq:angle

$$\alpha(p) = \cos^{-1} \frac{\|p - p^+\|^2 + \|p - p^-\|^2 - \|p^- - p^+\|^2}{2\,\|p - p^-\| \times \|p - p^+\|} \tag{3.2}$$

p is chosen as a control point, when α is less than a threshold T_α which is set to 150°. This is to make sure that two control points must be far apart. This also follows the constraint that the distance between any two control points must be larger than the threshold d_{min}. Between the close two candidates, p_1 and p_2 i.e., $|p_1 - p_2| \leq d_{min}$, the candidate with the smaller angle is chosen as a control point, shown in Figure 3.7(b).

In summary, the four steps of the algorithm to generate the constrained Delaunay triangulation are as follows:

1. Choose a starting edge $e\,(v_i, v_j)$ from the set of control points V extracted along the boundary of P as Figure 3.8.
2. Find the third vertex v_k of V that satisfies properties (i) and (ii).
3. Subdivide V into two sub-polygons: $V_a = \{v_i, v_k, v_{k+1}, ..., v_{i-1}, v_i\}$ and $V_b = \{v_j, v_{j+1}, ..., v_k, v_j\}$.
4. Repeat Steps 1-3 on and until the processed polygon consists of only one triangle.

After generating the triangle mesh, spanning tree is estimated from the center of each triangle in triangle mesh. The centroid is derived from parent nodes with more than one leaf of spanning tree. If there are more than one parent nodes, an averaging parent node point of body region as shown in Figure 3.6 or of foot region is used if the first one is absent. The centroid from triangle-based skeleton is able to capture features because delauney triangulation explores the shape of silhouette. If a shape is stretch out as arm, leg, or carried object the triangle mesh is generated through the shape creating the centroid at the joint point.

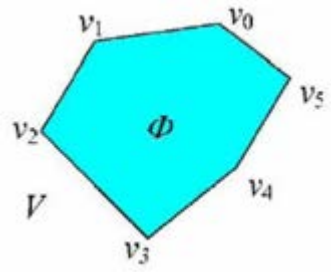

Figure 3.8: All the vertices are labeled anticlockwise such that the interior of V is located on their left.

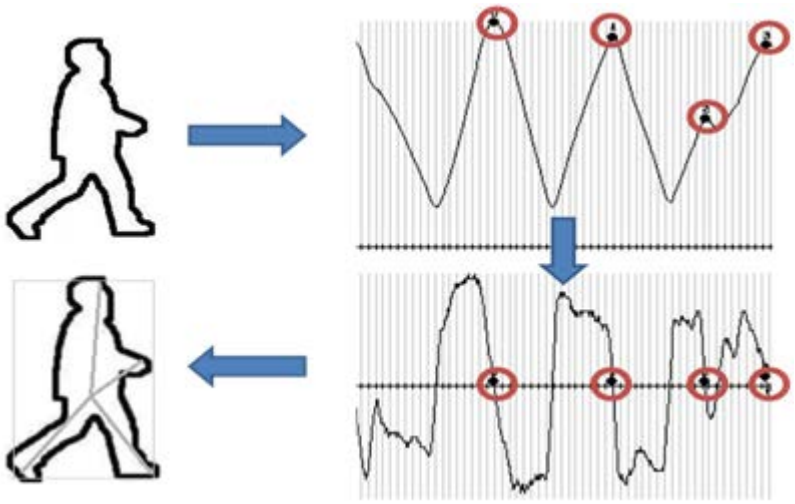

Figure 3.9: Process of star skeletonization

3.3 Star Skeletonization

A star skeleton for a human feature representation is computed according to the method proposed in (Chen et al., 2006). The distance from a centroid to each contour point is computed and expressed in one dimensional discrete function. The smoothing of distance series is performed to reduce noise by smoothing filter. Then local maximum or peak points of distance graph of distance series are identified by finding zero-crossings of the difference function as in Figure 3.9. The skeleton is constructed by joining the peak points to the centroid point. The limbs of star skeleton which are too close are excluded during the identification of local maximum points.

3.4 Tracking

At each frame in video, the computed limbs of a star skeleton are tracked using distance to the last frame's track and region of limb points as criteria. A tracked object gets a new track point which is in the same region and is the closest point among the computed limb points.

Figure 3.10: Demonstration of the difference of size due to the difference dimension

3.5 Normalizing the Tracked Position

Prior to the detection of a carried object, all track points need to be normalized because of the difference of depth. The size of human shape differs depending on the detected position in space. If it is near the camera it is large, otherwise it is small as demonstated in Figure 3.10.

To resolve this, the position of a tracked point P_i with height H_i at frame i is normalized to be relative to the reference height H_0 which is the track size at the first frame. The normalized position P_i' is determined as 3.3.

$$\begin{aligned} P_{i_x}^{'} &= P_{i_x} \times S_i \\ P_{i_y}^{'} &= P_{i_y} \times S_i \end{aligned} \tag{3.3}$$

where S_i denotes the scale size to normalize which is calculated from 3.4.

$$S_i = \frac{H_0}{H_i} \tag{3.4}$$

The normalized time series graph is as shown in Figure 3.11. Each line in graph is adjusted to be like in the same dimension and now steady lines can be observed.

3.6 Carried Object detection

A carried object is detected by accounting the x and y values of each tracked object's normalized position point in a period of time which can be represented by time series graphs in Figure 3.12. The graph of a tracked object which has low movement is classified to be a carried object.

The level of movement of each tracked object is determined by finding the mean difference

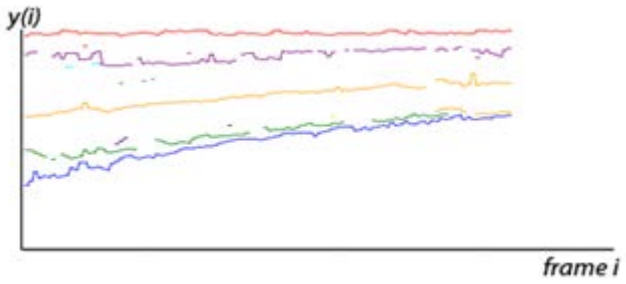

(a)

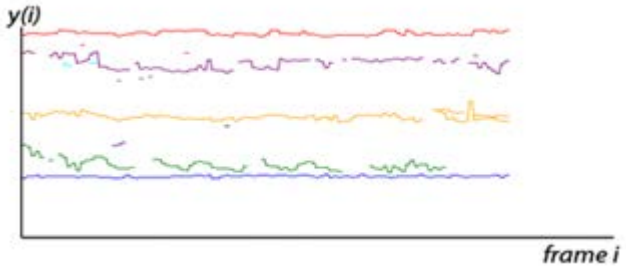

(b)

Figure 3.11: (a) Sample of time series graph of tracked position and (b) Time series graph of normalized tracked position

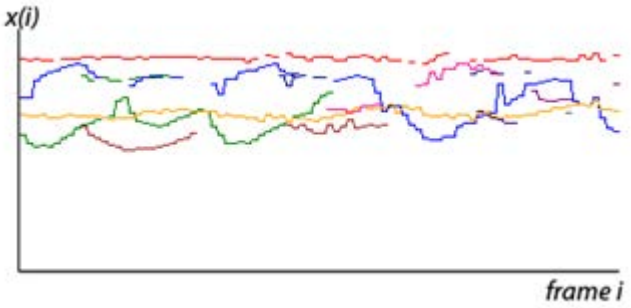

(a)

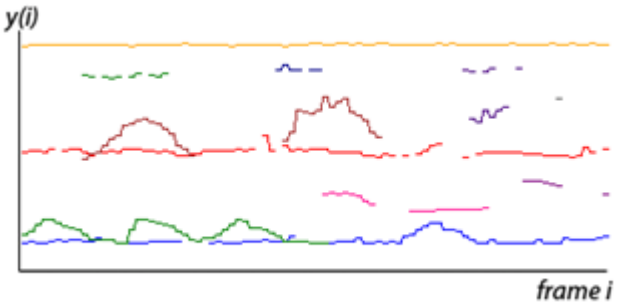

(b)

Figure 3.12: (a) Sample of time series graph of x value and (b) y value of tracked objects. Each line in graph is a tracked object. The movement and appearance of each tracked object can be observed from this graph

(a) (b)

Figure 3.13: (a) Limb points of triangle-based skeleton vary in a wide range from each frame while (b) limb points of star skeleton are more stable

of x and y values in the time series. If T_d is a threshold of the carried object classification and if the mean difference of x value and y value is lower than the threshold T_d then an object is classified as a carried object as 3.5:

$$A_{j_x} w + A_{j_y} (1 - w) < T_d \tag{3.5}$$

where A_{j_x} is the mean difference of x value and A_{j_y} is the mean difference of y value of tracked object j. The mean difference for n number of track points is calculated as follow equation 3.6:

$$\begin{aligned} A_{j_x} &= \tfrac{1}{n} \textstyle\sum_{i=1}^{n} \left| x_{j_i} - x_{j_{i-1}} \right| \\ A_{j_y} &= \tfrac{1}{n} \textstyle\sum_{i=1}^{n} \left| y_{j_i} - y_{j_{i-1}} \right| \end{aligned} \tag{3.6}$$

w is weight to concern whether x or y is more significant. In this case, x value is more significant due to the motions of arms and legs are easier observed and motions of carried objected should be low in x axis. Nevertheless, motions of carried objected in y axis is more noticeable as it follow human's horizontal movement when walking.

At the beginning of each track the mean difference is calculated from small number of track points which is not enough for accurate classification of a carried object, so some time threshold

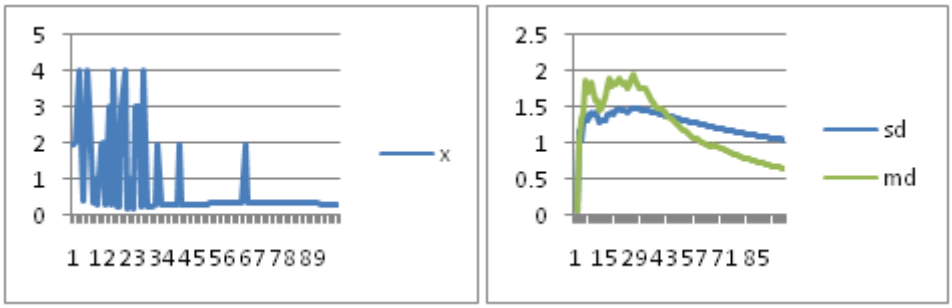

(a) (b)

Figure 3.14: In (b) Mean difference (green) and standard deviation (blue) usually be the same trend except in the case (a) where points are highly scattering

is set to constrain the carried object detector to wait for some period of time. When a silhouette is not moving, the carried object detector also pauses because most limb points would not be different. Nevertheless, the detected carried objects are still tracked for new track position. Each carried object is continually tracked until there is no track point for this object and the carried object's disappearance status is determined.

Although, triangle-based skeleton is extracted, it is not used because its limb points vary in a wide range from each frame causing high threshold of carried object detection, while the star skeleton is more stable as in Figure 3.13.

3.6.1 Time series

A time series is a sequence of data points, measured in time intervals which can be used to identify patterns in data. In this thesis, time series of normalized limbs' position of star skeleton is plotted and the limb with low average differences of time series would be a carried object. The leaving luggage event can be identified by the absence of the carried object track.

3.6.2 Mean difference and Standard deviation

At first, mean difference is used to measure the dispersion of position of limbs of star skeleton in time series graph. Therefore, there is other measurement of variability such as standard deviation. Compared to standard deviation, mean difference doesn't concern the central tendency while the standard deviation does.

In Figure 3.14 there are some cases that the graph of mean difference and standard devi-

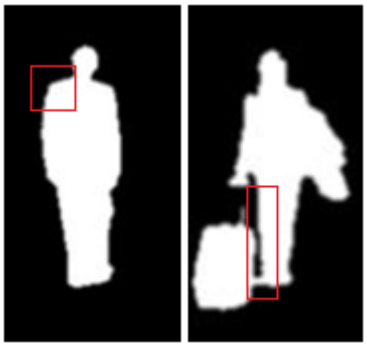

(a) (b)

Figure 3.15: (a) Failure of detecting shoulder and (b) leg as carried objects due to its steady signal in time-series graph.

ation are not follow the same trend, for example, a case that has high dispersion at first of the population and low at last. The mean difference reflect high value at first but low value at last, while the standard deviation is less affected. From this information, the standard deviation could be sometimes better than the mean different for judging how steady of graph especially for the sequences with high movement like running and with noise which could be from background segmentation process.

3.6.3 Area of consideration

Sometimes there is error in the detection of carried object which shoulders or legs are detected as carried object. This is because in some viewpoints star skeletonization sees a shoulder as limb object and it is naturally not moving, so the algorithm detects it as carried object. For legs, the front view of walking is occasionally hard to distinguish between leaf and right leg. The tracking algorithm sometimes confuse with left and right leg resulting the steady line in time series graph. This causes the detection of carried object to wrongly detect the leg as carried object as shown in Figure 3.15.

To avoid this problem, the area of consideration is used to exclude those areas of shoulder and legs from the concern of the detection algorithm. Therefore, areas considered for carried object detection are the middle body which expects backpack and the left and right side of lower body which expects luggage as shown in Figure 3.16.

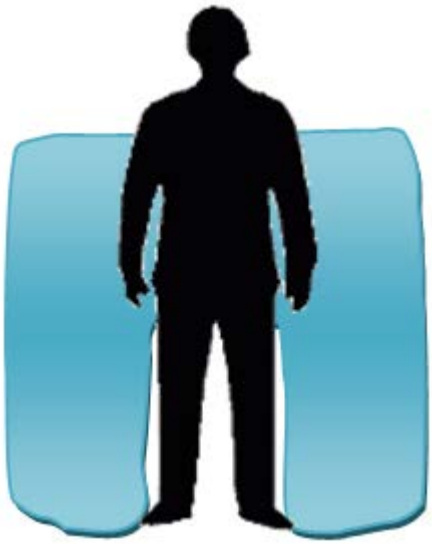

Figure 3.16: Areas around left and right of people (blue) exclude legs, shoulder and head are concerned

(a) (b) (c)

Figure 3.17: Failure of miss carried object detection due to the movement on y axis as (a) time series graph in x axis where the green line is carried object shows low movement whereas, (b) time series graph in y axis shows high movement. (c) MHi shows that area around a backpack is noticeable white.

3.6.4 Motion History Image

As the detection of carried objected is determined by motionless limbs of star skeleton, the carried object is assume to has little movement. The luggage is dragged on the floor so it's movement on the y axis or up and down is little and on the x axis is also little as people dragged it, whereas the backpack is difference. A backpack sticks with a person and is harder to determine with the same method as luggages as in Figure 3.17.

The improvement is done to be able to detect more backpack by using motion history image in the calculation. The motion history image is generated by accumulating the fraction of value

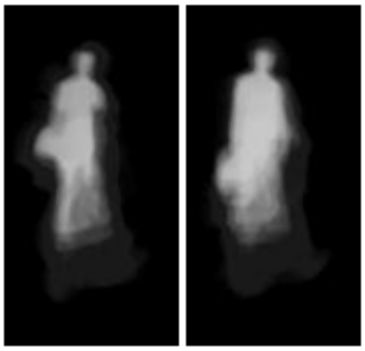

(a) (b)

Figure 3.18: Motion history image indicates area which is indifference with previous frames as brighter area and otherwise as darker area. In (a) and (b), backpack, briefcase and human body seem indifferent to the previous frames (brighter) while hands and legs are different (darker)

of foreground or shape of human in each frame. The area with high value, seen in image as white, is less difference to other frames', while the area with low value, seen in image as gray, change every frames. The motion history image (MHi) at frame f is generated follow the equation 3.7 by accumulating intensity of silhouette image I with weight α.

$$MHi_{i,j}(f) = \{MHi_{i,j}(f-1) + I_{i,j}(f) \cdot \alpha\} \cdot (1-\alpha) \tag{3.7}$$

The motion history image is used when a limb is failed to be carried object in the calculation. The values in motion history image of area around the limb's point are averaged to find whether it is carried object. If the average is high the result should be carried object as it has low difference from later frames, meaning it is motionless. Otherwise, it is not a carried object as shown in Figure 3.18.

This technique is used when the detection of carried object is fail using time-series graph. The technique is applied follow the equation 3.8.

$$MHi_{i,j}(f) > T_{MHi} \tag{3.8}$$

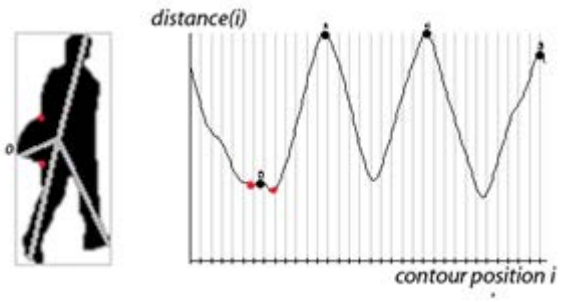

(a) (b)

Figure 3.19: (b) Sample of distance graph of star skeleton represent peak points with (a) adjacent sink curves to the carried object point in red and star skeleton with adjacent bottom points to the carried object point in red.

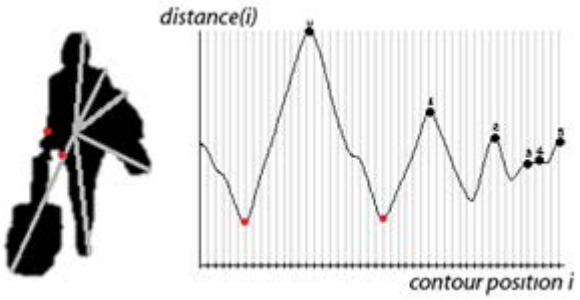

(a) (b)

Figure 3.20: (b) Another sample of distance graph of star skeleton represent peak points with (a) adjacent sink curves to the carried object point in red and star skeleton with adjacent bottom points to the carried object point in red.

3.7 Carried Object Boundary Approximation

The boundary of a detected carried object is figured from its current track points and adjacent sink curves of silhouette feature information. During star skeletonization, the peak points of a distance graph which are limbs of a star skeleton are extracted from zero-crossing of difference function from positive to negative. The bottom of a distance graph can also be extracted concurrently by zero-crossing of difference function from negative to positive. These bottom points are sink curves of the silhouette and two bottom points beside the current track peak point as shown in Figure 3.19 and Figure 3.20 are used in calculating rectangular boundary of a carried object.

CHAPTER IV

EXPERIMENTAL RESULTS

In this chapter, the experimental results are introduced. Results of experiments are computed from video sequences of walking people with luggage, backpack and without any carried objects obtained from video data of TRECVID dataset. The experiment is performed in 2 parts which are different in quality of video. Video sequences with perfect foreground extracted which is manually extracted are used to test the algorithm whether it is be able to detect the carried object. Then, with a background subtraction technique to get the foreground automatically, the algorithm is tested for its practicable usability.

4.1 Results from manually foreground extracted sequences

Experiments were performed on image sequences that have 320×240 pixel resolution and 25 frames per second. Video data of TRECVID dataset and manually captured data for leaving luggage event as shown in Figure 4.1 are used (Chayanurak et al., 2010). The method is tested with walking people with a luggage and a backpack and they were successfully detected and tracked. The carried object boundary then was well approximated for the result presentation. Detection of the leaving luggage event in the capture video is able to achieve as shown in Figure 4.2. Figure 4.2(a,b,c) represents silhouette of a person leaving a luggage. Figure 4.2(d,e) represents time series graph of x and y value where a line in each graph with bold and black color represents the carried object status. The black line stop at a frame where the track object is missing or the luggage is left. Sample results of method are shown in Figure 4.3.

In conclusion, the algorithm can be used to detect carried objects and identify the discon-

(a) (b)

Figure 4.1: (a) Samples of TRECVID dataset and (b) manually captured data

(a) (b) (c)

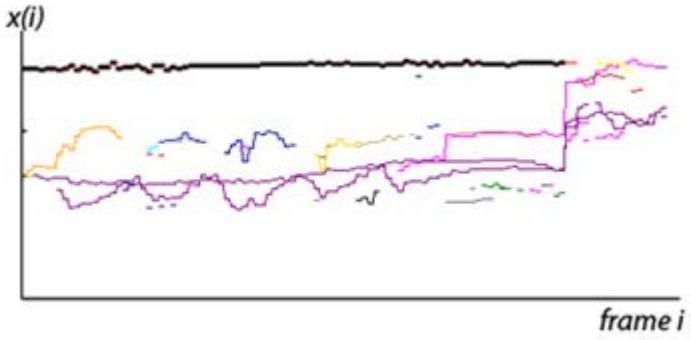

(d)

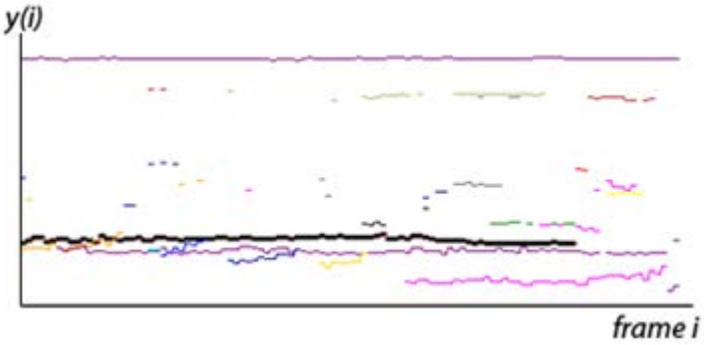

(e)

Figure 4.2: (a) Detection of luggage during the leaving luggage event, (b) walking with luggage, (c) stop walking and starting to leave the luggage, leaving the luggage; Movement of tracked objects is shown in (d) time series graph of x value and (e) y value.

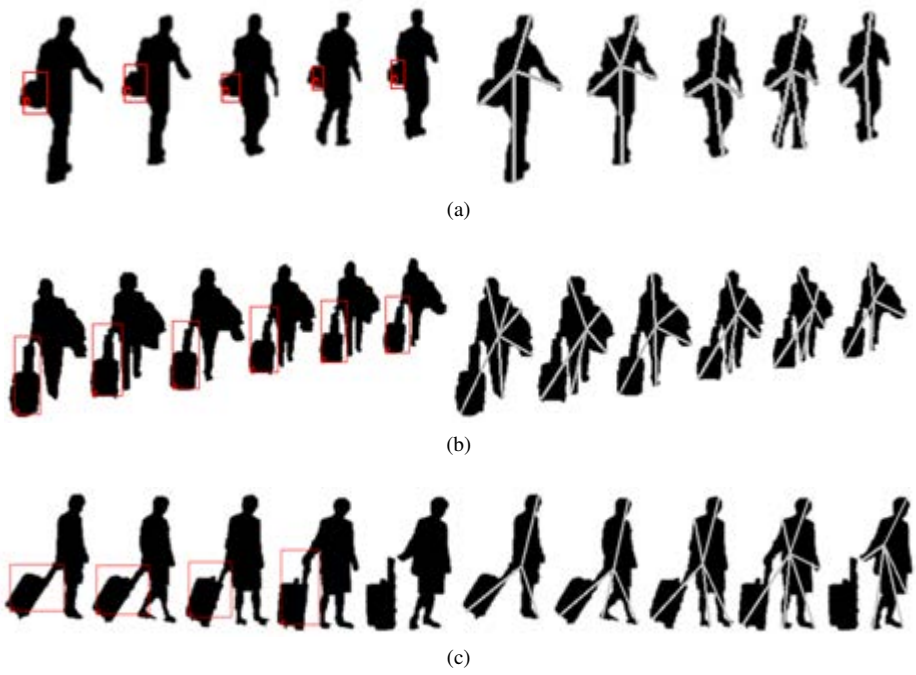

(a)

(b)

(c)

Figure 4.3: Results of sample video sequences. (a) A person walking with a backpack. (b) A person walking with a luggage. (c) A person walking with a luggage and leaving the luggage.

necting of carried object and its carrier.

4.2 Results from automatically foreground extracted sequences

The previous results are that from manually background subtraction which the silhouettes are always complete. Therefore silhouettes from automatically background subtraction are sometimes incomplete. Some extracted silhouette can be used some can't be distinguished clearly. Note that the background subtraction technique used in this experiment is that follow the algorithm in (Kasamwattanarote et al., 2012).

Figures in Table 4.1 are some example sequences of silhouettes from automatically background subtraction, and the method could be able to extract star skeleton and detect the carried object. They show various results which indicate cases that the method can detect. More than one carried objects can be detected and whether it is carried on left or right.

To evaluate the result is to determine whether the human justification is the same as the result from the algorithm. Begin with a silhouette from background segmentation process, if human can detect the carried object the result from algorithm is also expected to be able to detect. However, if the human can't detect, it is ok for the algorithm to fail detecting any carried object

Table 4.1: Samples of correctly detection of carried object.

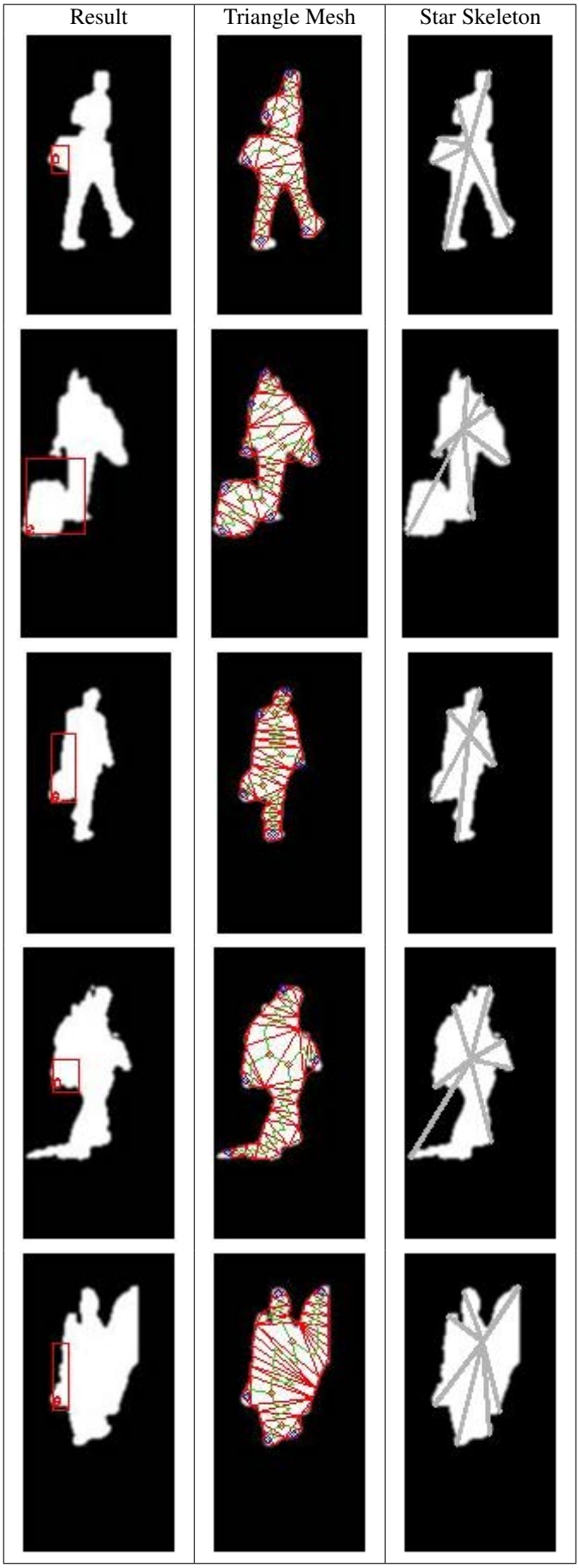

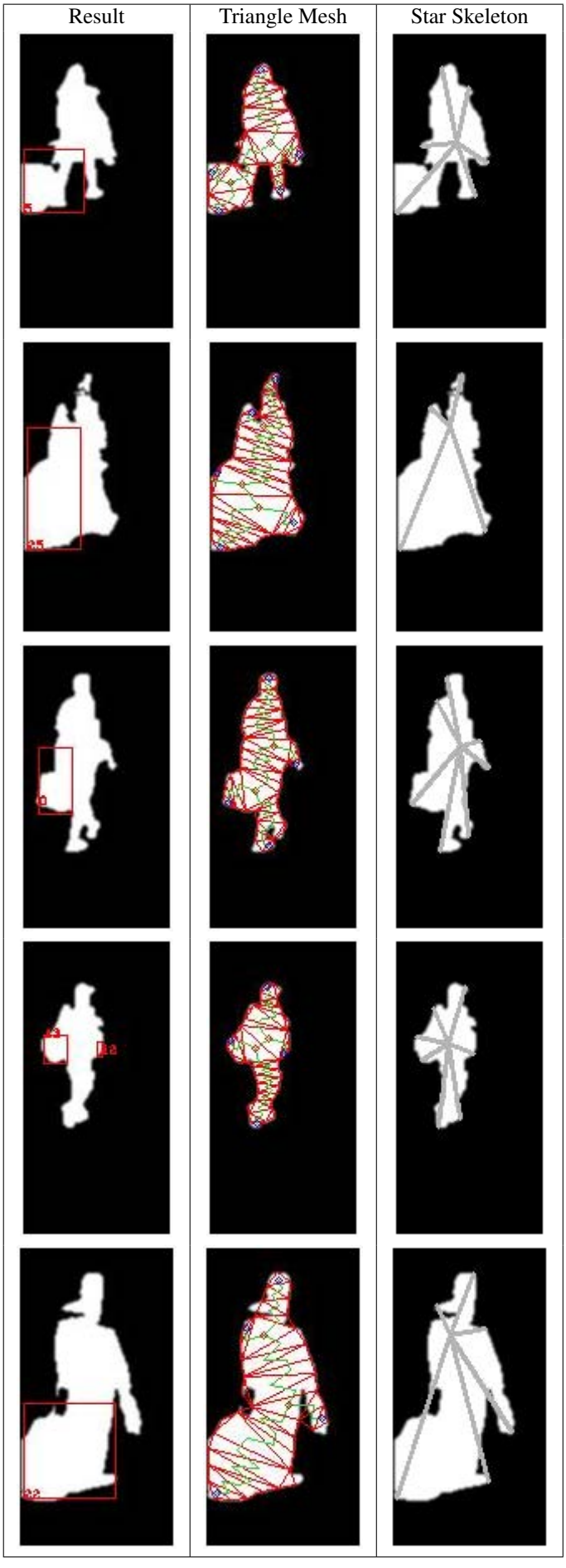
Result
Triangle Mesh
Star Skeleton

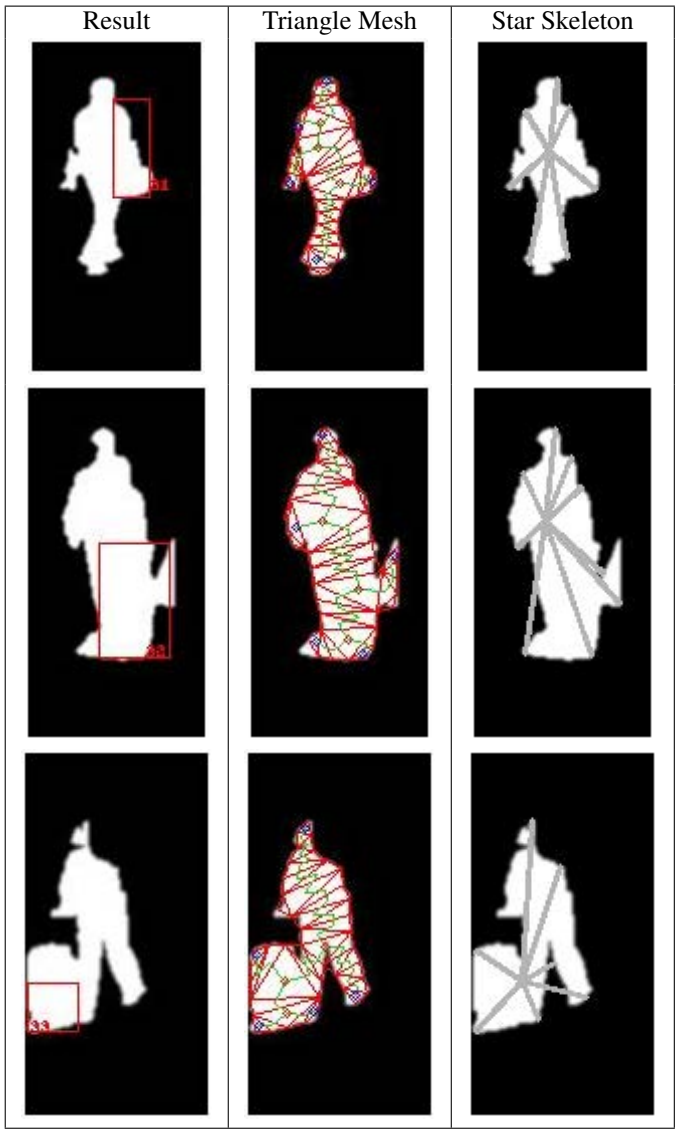
Result
Triangle Mesh
Star Skeleton

Table 4.2: Confusion matrix for carried object detection

		Predicted	
		Negative	Positive
Actual	Negative	6	4
	Positive	2	27

from the same sequence.

From 39 testing sequences which their foregrounds are automatically extracted, carried object in 33 are correctly identified by the algorithm as shown in Table 4.2.

Example 1: True positive case, a sequence with carried object and carried object predicted is consider. Figure 4.4(a) shows a example sequence that results as this case. The method can performed detection correctly due to the stable limb's positions in graph as in Figure 4.4(b) , where pink line represents the carried object.

Example 2: True negative case, a sequence with no carried object and carried object not predicted is consider. Figure 4.5(a) shows a example sequence that results as this case. As in Figure 4.5(b), all line in the graph are not steady in both x and y axis, except the line representing the head.

Example 3: False positive case, a sequence with no carried object and carried object predicted is consider. Figure 4.6(a) shows a example sequence that results as this case. There is a low dispersion value of a limb's as in Figure 4.6(b), the black represents the wrong detected carried object, detecting the coat instead. It may be because some limb signals are not continuous reflecting the lower variance value.

Example 4: False negative case, a sequence with carried object and carried object not predicted is consider. Figure 4.7(a) shows a example sequence that results as this case. In Figure 4.7(b), all line in the graph are unstable in both x and y axis, also the MHi could help because of the incompleteness in some frames.

4.3 Improvement by Standard deviation, Area of consideration and Motion History image

At first, with the same method used in the manually foreground extracted sequences could not properly perform well due to the incompleteness of data. There are some improvements that in chapter III has described about.

(a)

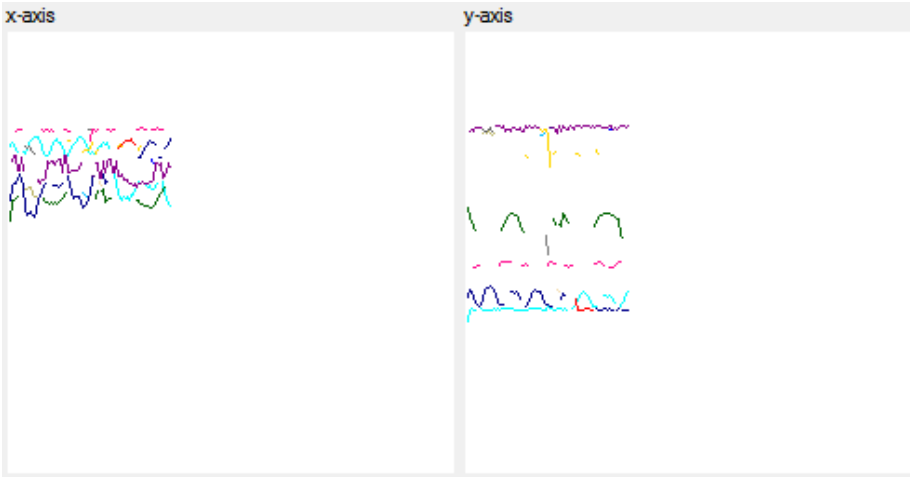

(b)

Figure 4.4: (a) Sample video sequence with true positive result with (b) its time series graph

(a)

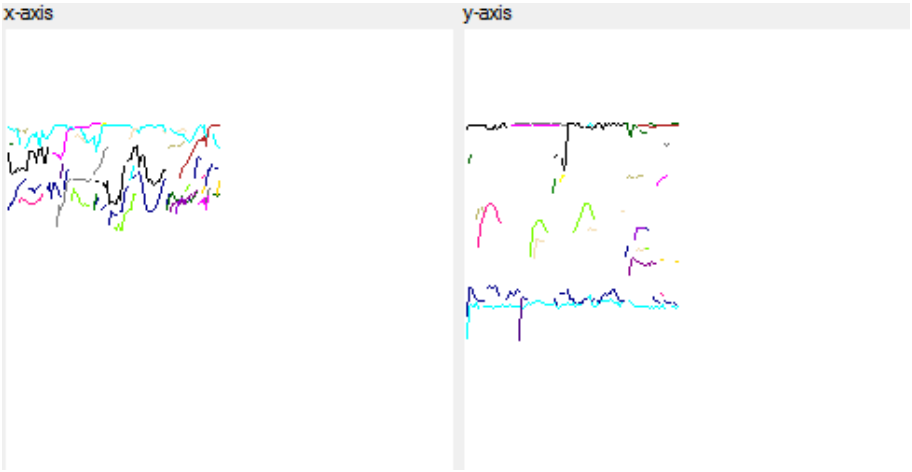

(b)

Figure 4.5: (a) Sample video sequence with true negative result with (b) its time series graph

(a)

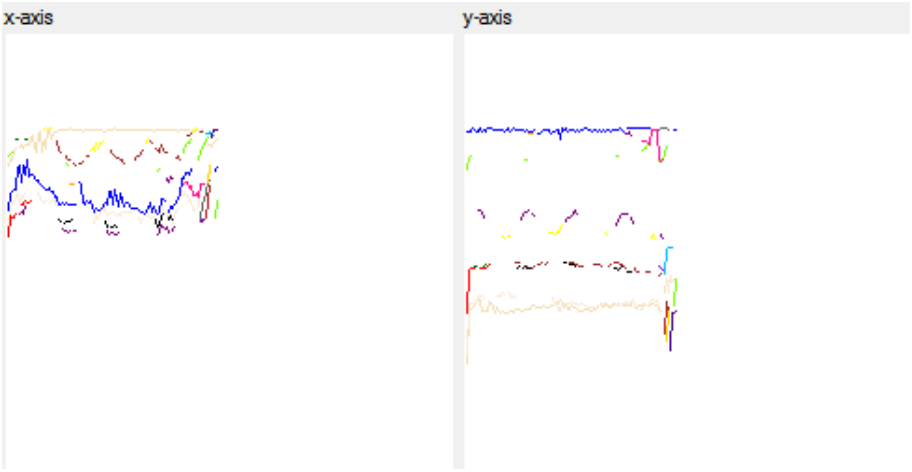

(b)

Figure 4.6: (a) Sample video sequence with false positive result with (b) its time series graph

(a)

(b)

Figure 4.7: (a) Sample video sequence with false negative result with (b) its time series graph

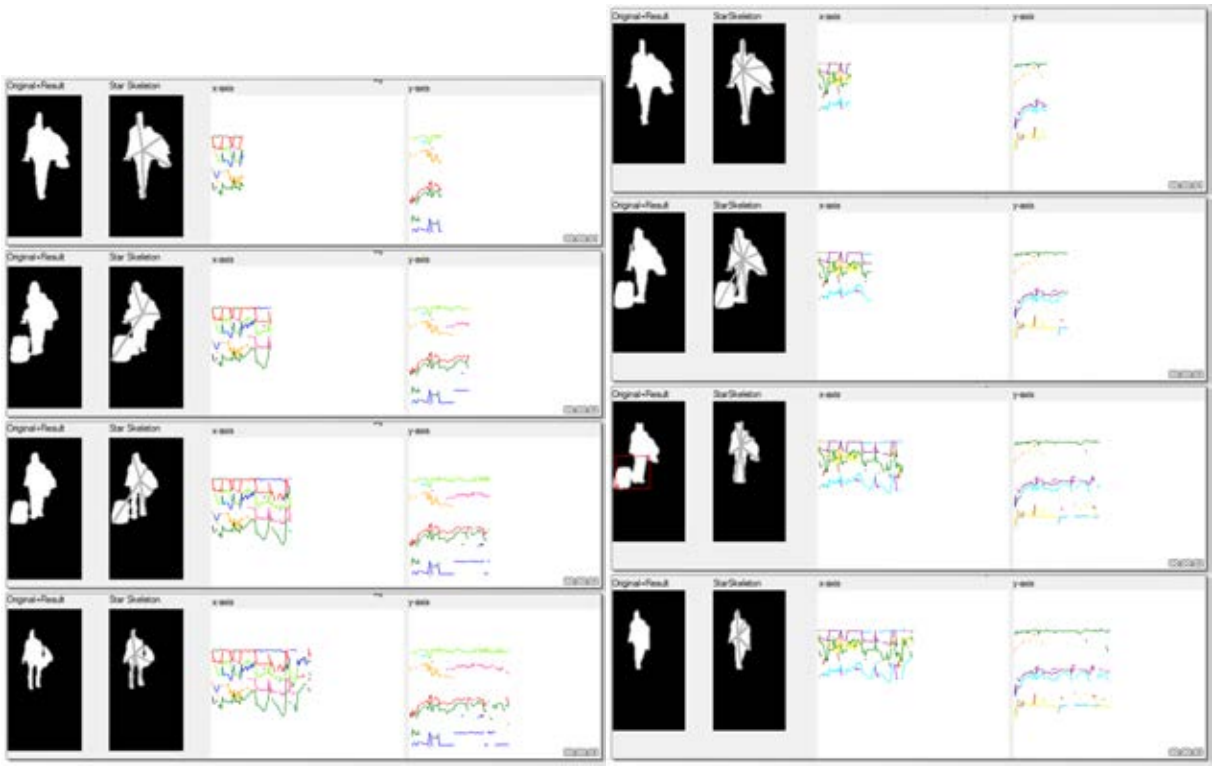

(a) (b)

Figure 4.8: (a) Sample video sequence with result using mean difference and (b) the same one using standard deviation

The first try of improvement is to change the method to calculate the dispersion from mean difference to standard deviation, which is sometimes better than the mean different for judging how steady in sequences with high movement like in the case that data is fragmented and become improperly tracked causing unstable of graph signal. Figure 4.8 displays an example that the method with standard deviation calculating the dispersion could able to detect the carried object while the mean difference could not.

Another improvement is to use Area of consideration and Motion History image that also is described in chapter III and the results are satisfaction as in 4.9 that it is able to correctly detect backpack. In more details, for each tracked limb, when its dispersion value exceeds the threshold, but still not too high, the method then look at its motion history image at its tracked point. Then average the intensity value nearby the limb point and if it is smaller than the threshold, a new carried object is detected.

Figure 4.11 shows that using standard deviation to measure the dispersion results the better

(a) (b)

Figure 4.9: (a) Sample video sequence without Area of consideration and Motion History image and (b) the same one with Area of consideration and Motion History image

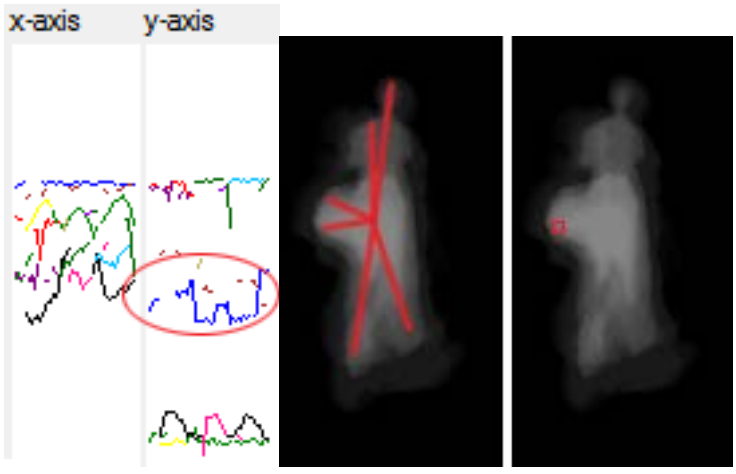

(a) (b)

Figure 4.10: Steps of using Motion History image when (a) the (blue) line of limb represented carried object is not steady and the method look at (b) its MHi at the position where the end point of limb is.

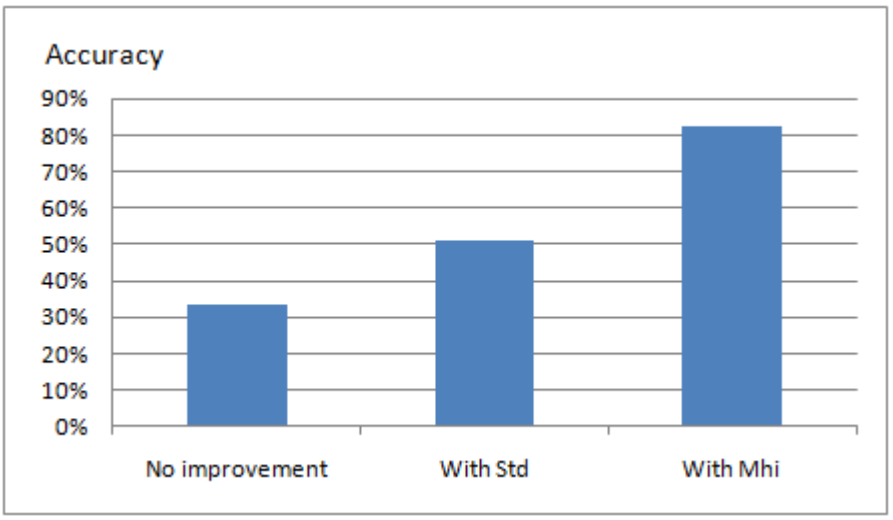

Figure 4.11: Percentage of correct results from algorithm with no improvement, Standard deviation, Area of consideration and Motion History image

correctness of detection. And also there are more carried object detected with Area of consideration and Motion History image and also prevention of wrong detection.

Furthermore, there are also some tries that is incapable to significantly improve the method. One is to try to improve the tracking by limiting the next tracking point to be in some area around the previous one, however this fail to prevent the wrong tracking when 2 signals cross such as left and right legs. Perhaps, the whole signal history should be used instead of just a previous one. Trying to improve the detection of backpack by increasing the number of limbs of created star skeleton is also unsatiably and even cause more mistakes. Therefore, it is not because skeleton that making the backpack to be difficult to detect but the higher motion of track signal than the luggage and the incompleteness of human silhouette. The proper improvement sometimes should be method that is robust to the incomplete data.

Lastly, the results are satisfactory for carried object detection in video sequences as second part which foregrounds are imperfectly extracted. However, to identify the disconnecting of carried object and its carrier is still impractical because of the incomplete foreground extracted. As sometime the foreground is incomplete or missing from sequences making the tracking mechanism fails to track the carried object signal and sometimes make a wrong justification, so it is not practical. Some improvement of foreground extracting would improve the result.

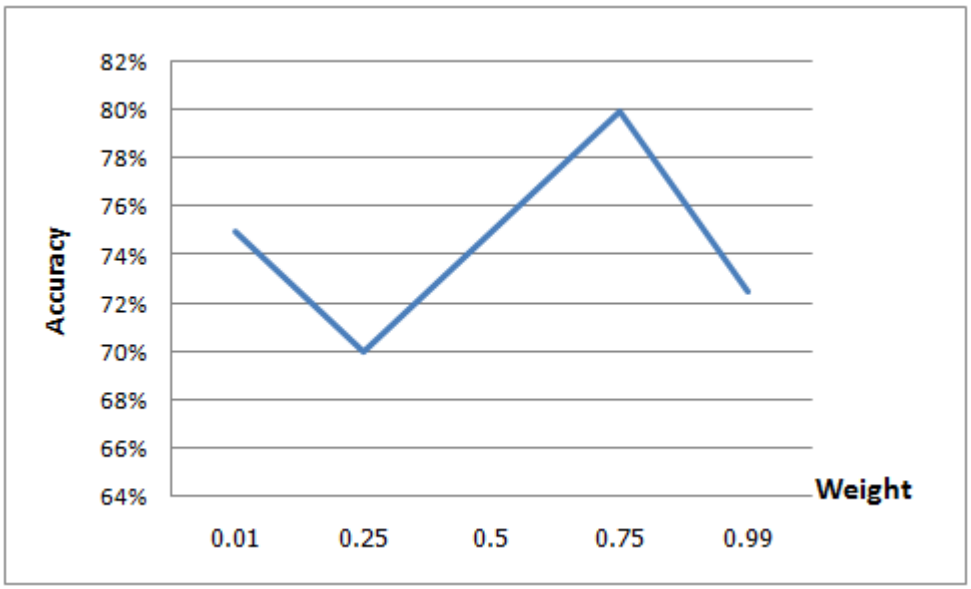

Figure 4.12: Accuracy of results with different weight compared

4.4 Weight Parameter

From chapter III the equation 3.5 which about to determine the carried object, weight parameter indicates the concentration on whether the motion horizontally or vertically(x or y). However, the question is that is x or y should be concerned. In this experiment, x value is more concerned due to the hypothesis that the carried object should not be swang so that movements of arms and legs are significant compare to the carried object. Nevertheless, in real situation may not be as the above, so this section the accuracy of results with different weight are compared as shown in Figure 4.12.

The comparison shows that with weight .75 results highest accuracy, therefore, the different to other are still small. The interesting issue is that whether x or y is used, there are some cases that always given correct result, some luggage cases. For weight .01, it corrects more undetected carried object that other weights don't, but more mistake in on carried object sequences. In conclusion, adaptive weight may be better, if the result is adequate compare to the increase in processing time for compute weight.

4.5 Threshold Parameter

From chapter III the equation 3.5 which about to determine the carried object, threshold parameter classified the carried object. The accuracy of results with different threshold are compared

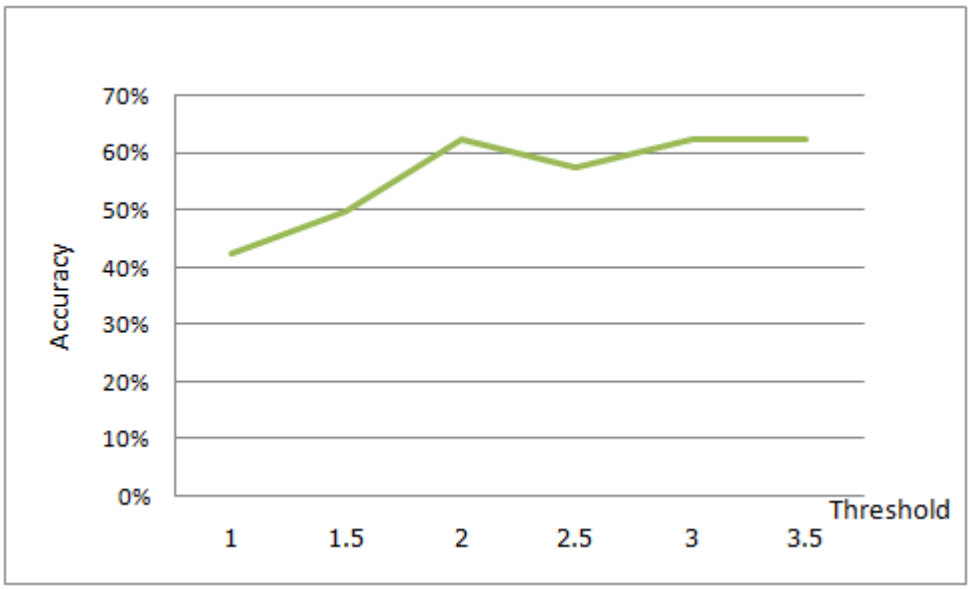

Figure 4.13: Accuracy of results with different threshold compared

in this section as shown in Figure 4.13.

The comparison implies that increasing the weight to some points does not obviously effect the accuracy. Therefore, the higher false positive cases occurs.

4.6 Video captured in other view point

There are some difficulties with sequences captured in other view point. As in Figure 4.14, the camera's position is quite higher than camera's position capturing the test sequences. The failure occurs in tracking process when a leg is confused with a luggage resulting the line representing the leg become the luggage. Therefore, the luggage is not detected. This situation arises in the sequence captured in higher view point, where the testing model is not entirely applicable especially the area of consideration. In the testing model the area of consideration concerns only human shapes in front view where the silhouette in this view quite inclines thus there are some chances that a leg can wrongly enter the area of consideration.

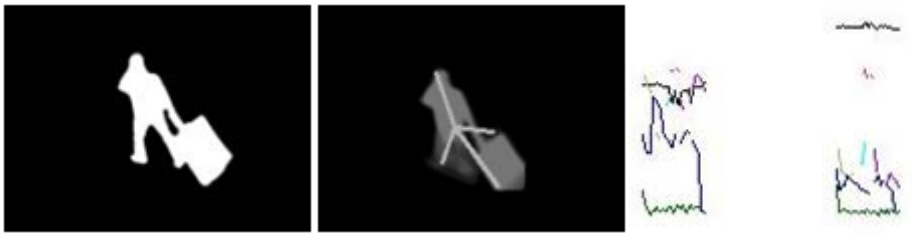

(a) (b) (c) (d)

Figure 4.14: (a) A sample silhouette of sequences captured in other view point and (b) extracted star skeleton with motion image. (c)Time series graph of x value and (d) y value of this sample silhouette.

CHAPTER V

CONCLUSIONS AND FUTURE WORKS

5.1 Conclusion

A method for carried object detection and tracking is proposed. Star skeleton is used to represent feature of human postures. The time series graph is used to determine if a track limb of a star skeleton is a carried object. Because of the normalization of limb's positions, the detection can be done in view where the carried object isn't totally occluded. A backpack and a luggage with walking human and the leaving luggage event are successfully detected. Therefore, the identification of leave luggage event could not be accomplished due to the incompletion of the extracted silhouettes. Also sequences in different view point could not be able to detect the carried object by the algorithm. Moreover the area of consideration and motion history image are introduced to improve the correctness of detection.

5.2 Future Works

This work needs robust foreground segmentation as it depends mainly on silhouette information. The proposed method could be improved by advance tracking method for tracking the position of limbs' of star skeleton and movement calculation.

References

Brian DeCann and Arun Ross. 2010. Gait curves for human recognition, backpack detection and silhouette correction in a nighttime environment. In SPIE Conference on Biometric Technology for Human Identification VII, Orlando, USA.

Chiraz BenAbdelkader and Larry Davis. 2002. Detection of people carrying objects : a motion-based recognition approach. In IEEE International Conference on Automatic Face and Gesture Recognition, pp. 378 – 383, Washington, DC, USA.

Chan su Lee and Ahmed Elgammal. 2006. Carrying object detection using pose preserving dynamic shape models. In Conference on Articulated Motion and Deformable Objects, pp. 315–325.

Chi-Hung Chuang, Jun-Wei Hsieh, Luo-Wei Tsai, and Kuo-Chin Fan. 2008. Human action recognition using star templates and delaunay triangulation. In International Conference on Intelligent Information Hiding and Multimedia Signal Processing, pp. 179–182, Harbin.

Chi-Hung Chuang, Jun-Wei Hsieh, Luo-Wei Tsai, Sin-Yu Chen, and Kuo-Chin Fan. 2009. Carried object detection using ratio histogram and its application to suspicious event analysis. IEEE Transactions on Circuits and Systems for Video Technology 19,6:911–916.

Dima Damen and David Hogg. 2008. Detecting carried objects in short video sequences. In European Conference on Computer Vision, pp. 154–167, Marseille, France.

Elden Yu and Jake K. Aggarwal. 2006. Detection of fence climbing from monocular video. In International Conference on Pattern Recognition, pp. 375–378.

Hsuan-Sheng Chen, Hua-Tsung Chen, Yi-Wen Chen, and Suh-Yin Lee. 2006. Human action recognition using star skeleton. In ACM international workshop on Video surveillance and sensor networks, pp. 171–178, Santa Barbara, California, USA.

Ismail Haritaoglu, Ross Cutler, David Harwood, and Larry S. Davis. 1999. Backpack: Detection of people carrying objects using silhouettes. In International Conference on Computer Vision, p. 102, Corfu, Greece.

John Canny. 1986. A computational approach to edge detection. IEEE Transactions Pattern Analysis and Machine Intelligence PAMI-8,6:679 – 698.

Siriwat Kasamwattanarote, Nagul Cooharojananone, Shin'ichi Satoh, and Rajalida Lipikorn. 2012. Automated real-time video surveillance summarization framework. Journal of Real-Time Image Processing .

L. Paul Chew. 1987. Constrained delaunay triangulations. In Symposium on Computational geometry, pp. 215–222, Waterloo, Ontario, Canada.

Milan Petkovic, Willem Jonker, and Zoran Zivkovic. 2001. Recognizing stokes in tennis videos using hidden markov models. In Proceeding of Intl. Conf. on Visualization, Waterloo, Ontario, Canada.

Narongsak Putpuek, Nagul Cooharojananone, and Chidchanok Lursinsap. 2007. Complex human motions analysis using an adaptive star skeleton. In International Conference on Advances in Information Technology.

Yue Qi, Guo-Chang Huang, and Yun-Hong Wang. 2007. Carrying object detection and tracking based on body main axis. In International Conference on Wavelet Analysis and Pattern Recognition, pp. 1237 – 1240, Beijing, China.

R. Venkatesh Babu and Kalpathi R. Ramakrishnan. 2004. Recognition of human actions using motion history information extracted from the compressed video. Image and Vision Computing 22,8:597–607.

Rawin Chayanurak, Nagul Cooharojananone, Shin'ichi Satoh, and Rajalida Lipikorn. 2010. Carried object detection using star skeleton with adaptive centroid and time series graph. In International Conference on Signal Processing, pp. 736–739, Beijing, China.

Tobias Senst, Ruben Heras Evangelio, Volker Eiselein, Michael Pätzold, and Thomas Sikora. 2010. Towards detecting people carrying objects - a periodicity dependency pattern approach. In International Conference on Computer Vision Theory and Applications, pp. 524–529, Angers, France.

Vicente Luis Atienza Vanacloig and Jose Miguel Valiente-González Juan Alfonso Rosell Ortega, Gabriela Andreu García. 2008. People and luggage recognition in airport surveillance under real-time constraints. In International Conference on Pattern Recognition, pp. 1–4, Tampa, Florida, USA.

APPENDIX

APPENDIX A

RESULTS

This section displays results obtained from the proposed method as discussed in chapter 4. There are 39 sequences of silhouette extracted from video data of TRECVID dataset. Results are represented in 3 images captured in 3 different time in sequences and their time series graph as shown in following figures.

Seq.1	t1 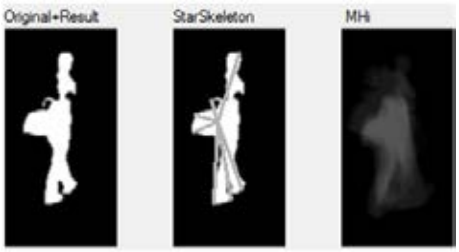 t2 t3 	time series graph
Seq.2	t1 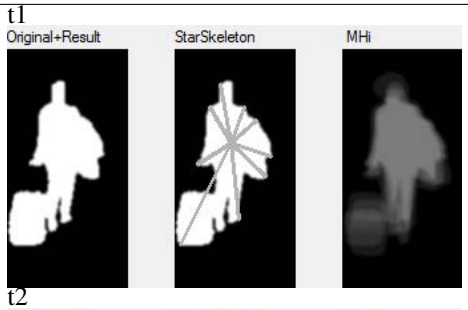 t2 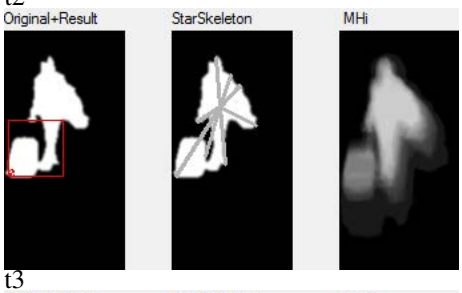 t3 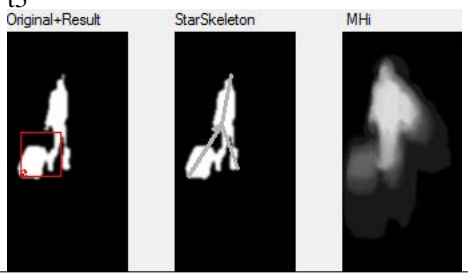	time series graph 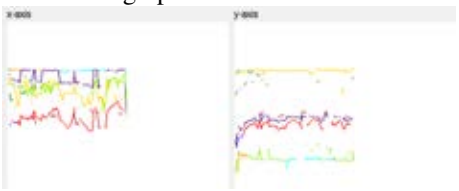

Seq.3	t1 t2 t3 	time series graph 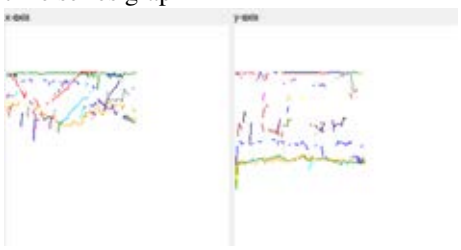
Seq.4	t1 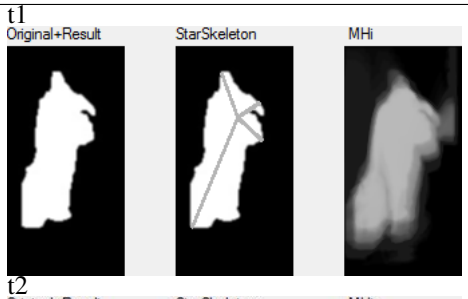 t2 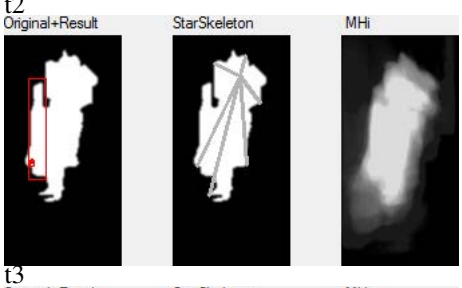 t3 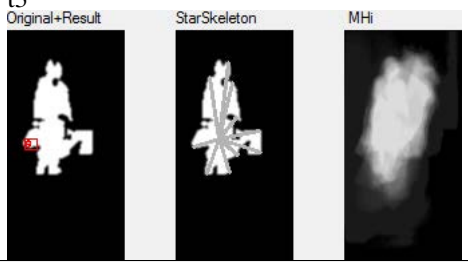	time series graph

Seq.5	t1 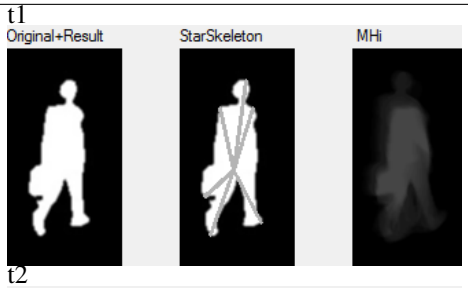 t2 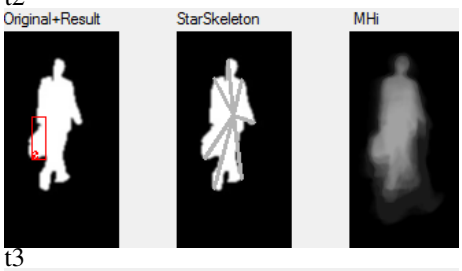 t3 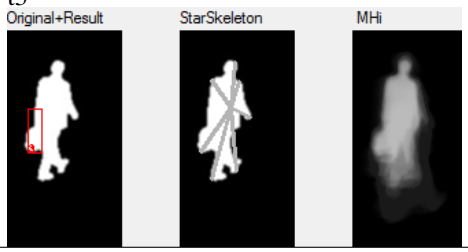	time series graph
Seq.6	t1 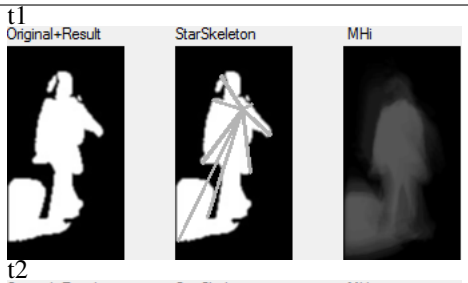 t2 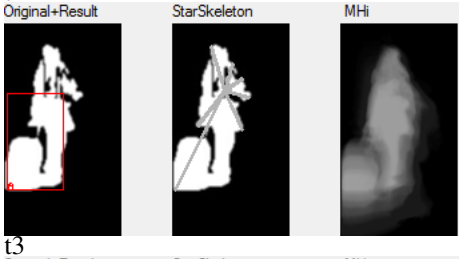 t3 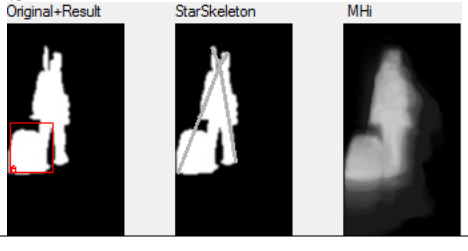	time series graph 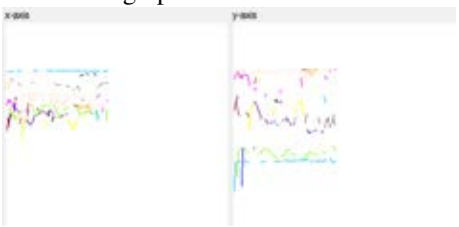

Seq.7	t1 Original+Result StarSkeleton MHi 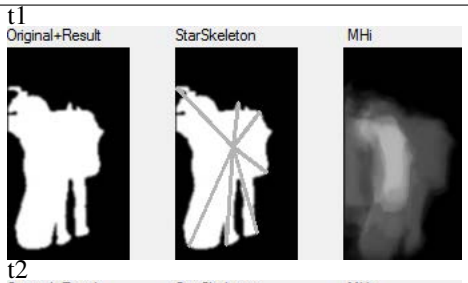 t2 Original+Result StarSkeleton MHi 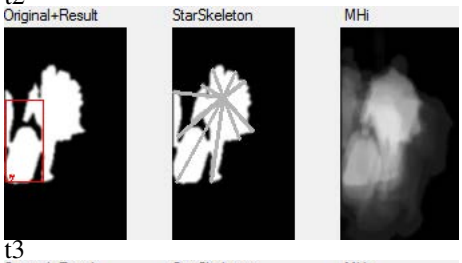 t3 Original+Result StarSkeleton MHi 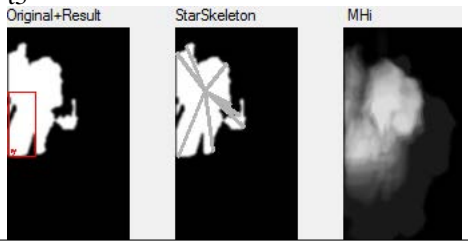	time series graph 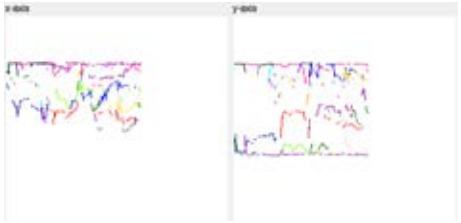
Seq.8	t1 Original+Result StarSkeleton MHi 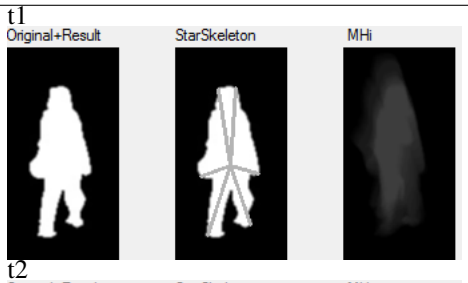 t2 Original+Result StarSkeleton MHi t3 Original+Result StarSkeleton MHi 	time series graph 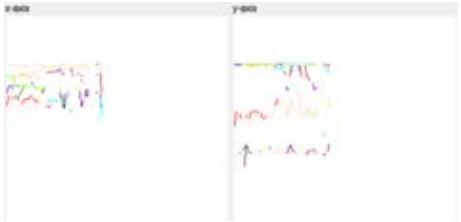

Seq.9	t1 Original+Result StarSkeleton MHi 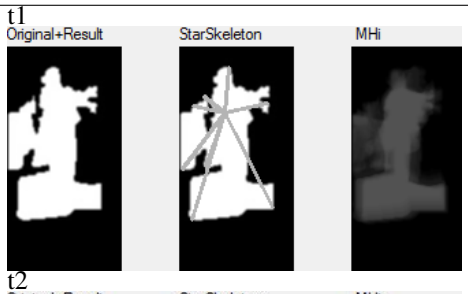 t2 Original+Result StarSkeleton MHi t3 Original+Result StarSkeleton MHi 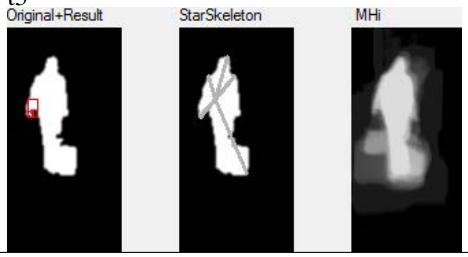	time series graph 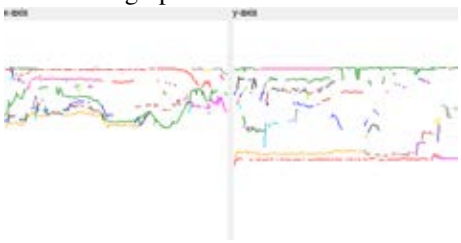
Seq.10	t1 Original+Result StarSkeleton MHi 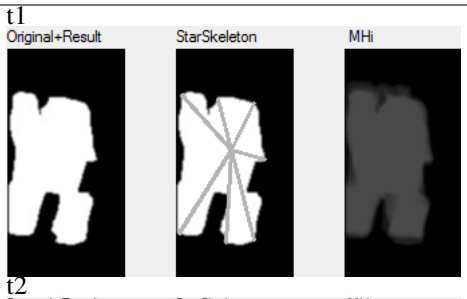 t2 Original+Result StarSkeleton MHi 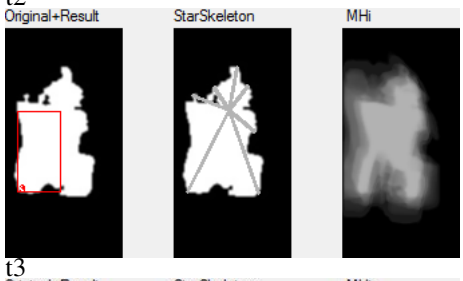 t3 Original+Result StarSkeleton MHi 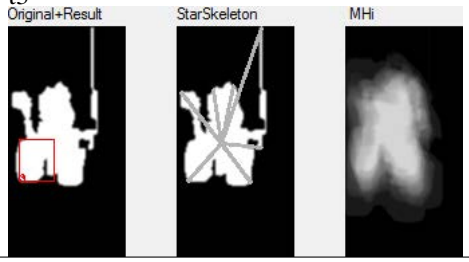	time series graph 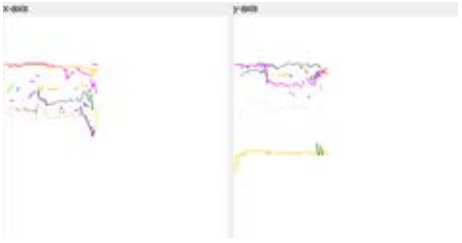

Seq.11	t1 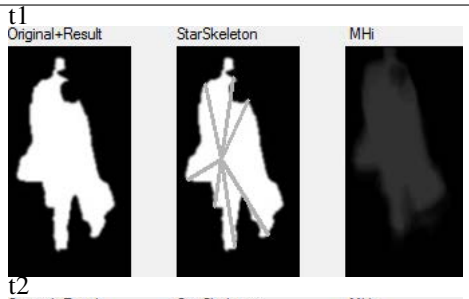 t2 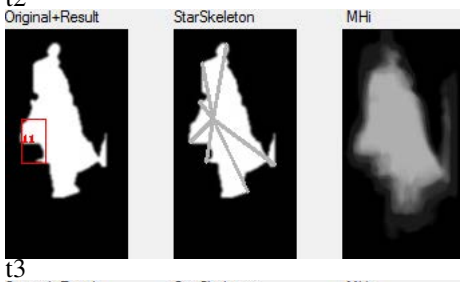 t3 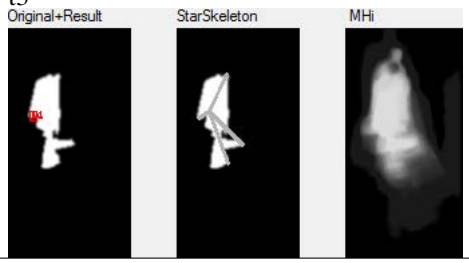	time series graph 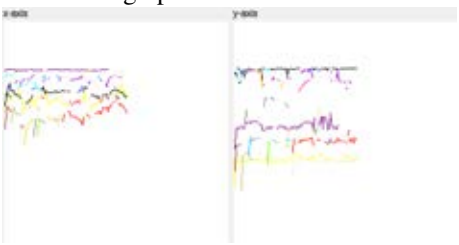
Seq.12	t1 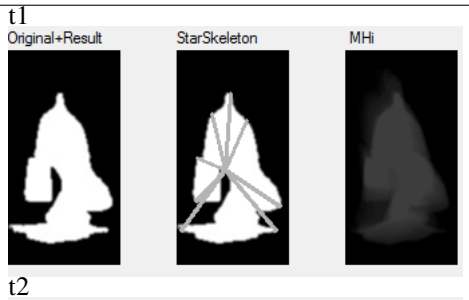 t2 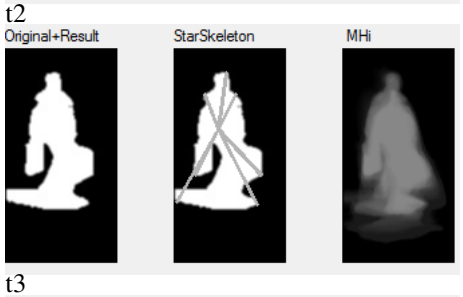 t3 	time series graph 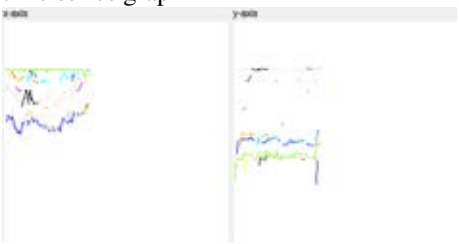

Seq.13	t1 Original+Result StarSkeleton MHi t2 Original+Result StarSkeleton MHi t3 Original+Result StarSkeleton MHi	time series graph x-axis y-axis
Seq.14	t1 Original+Result StarSkeleton MHi t2 Original+Result StarSkeleton MHi t3 Original+Result StarSkeleton MHi	time series graph x-axis y-axis

Seq.15	t1 Original+Result StarSkeleton MHi 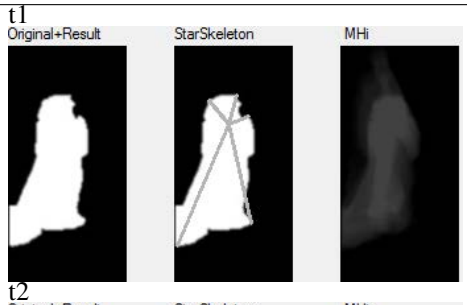 t2 Original+Result StarSkeleton MHi 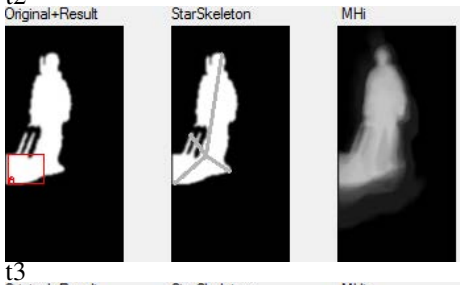 t3 Original+Result StarSkeleton MHi 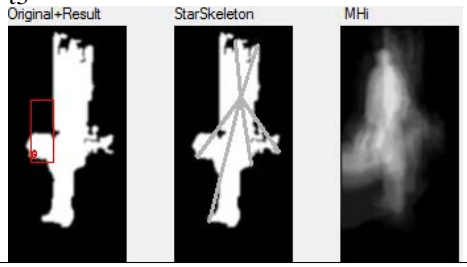	time series graph 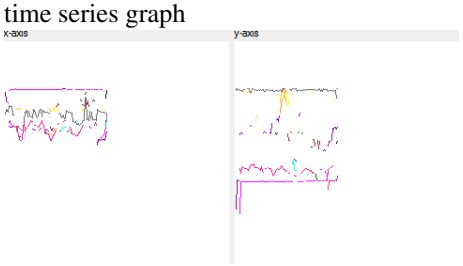
Seq.16	t1 Original+Result StarSkeleton MHi 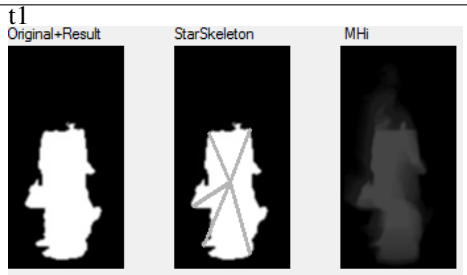 t2 Original+Result StarSkeleton MHi t3 Original+Result StarSkeleton MHi 	time series graph

Seq.17	t1 Original+Result StarSkeleton MHi 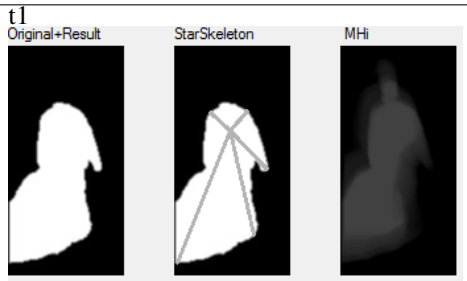 t2 Original+Result StarSkeleton MHi t3 Original+Result StarSkeleton MHi 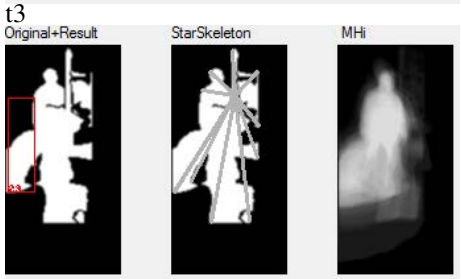	time series graph
Seq.18	t1 Original+Result StarSkeleton MHi t2 Original+Result StarSkeleton MHi 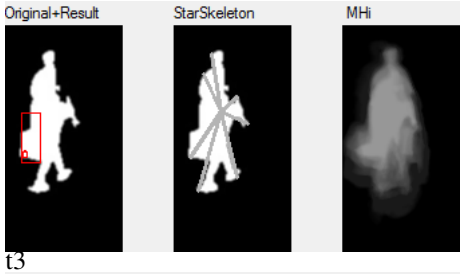 t3 Original+Result StarSkeleton MHi 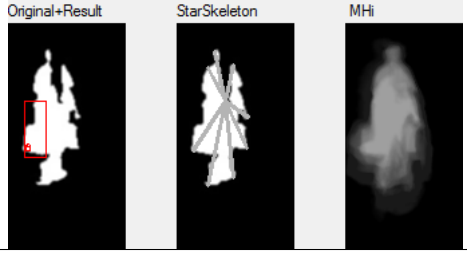	time series graph

Seq.19	t1 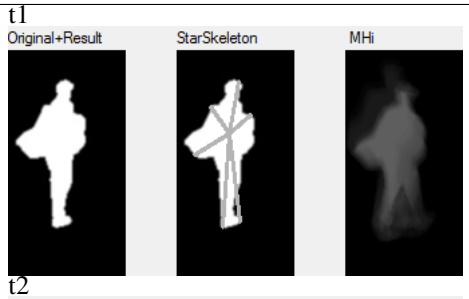 t2 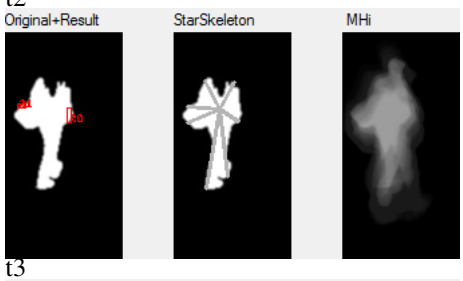 t3 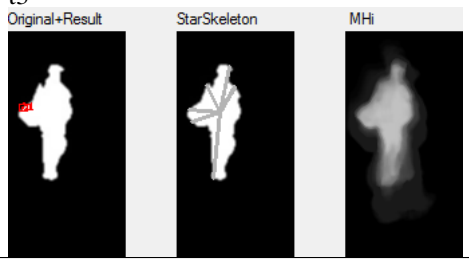	time series graph 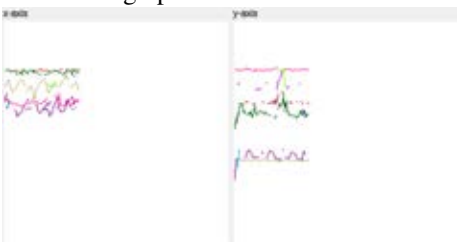
Seq.20	t1 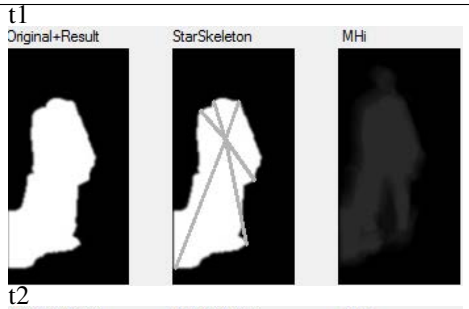 t2 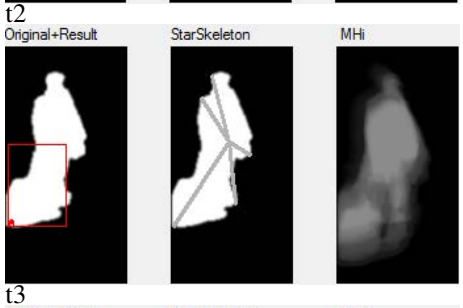 t3 	time series graph 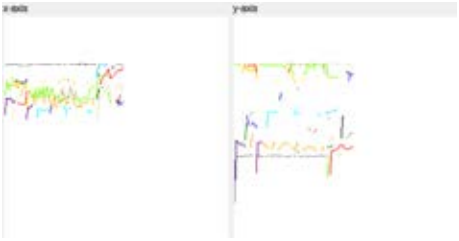

Seq.21	t1 Original+Result StarSkeleton MHi 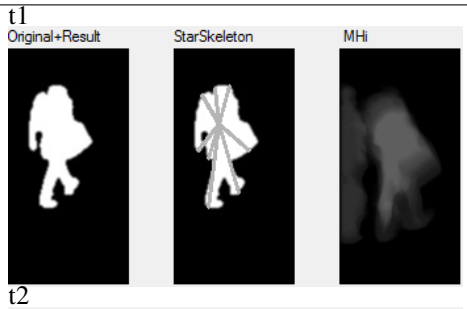 t2 Original+Result StarSkeleton MHi 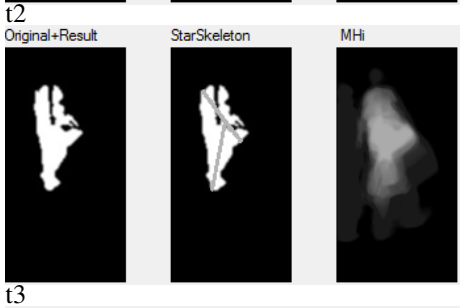 t3 Original+Result StarSkeleton MHi 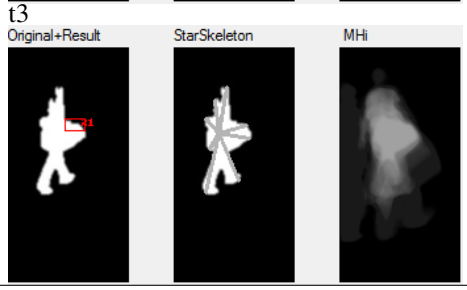	time series graph
Seq.22	t1 Original+Result StarSkeleton MHi 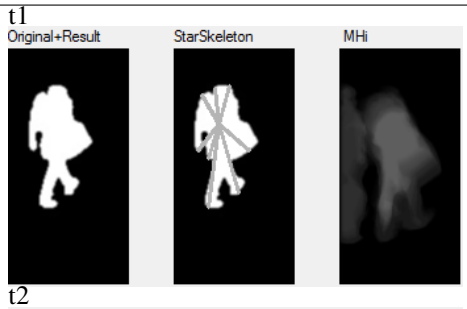 t2 Original+Result StarSkeleton MHi t3 Original+Result StarSkeleton MHi 	time series graph 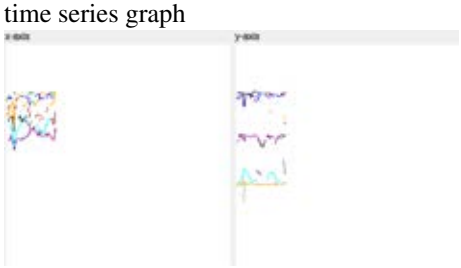

Seq.23	t1 Original+Result StarSkeleton MHi t2 Original+Result StarSkeleton MHi 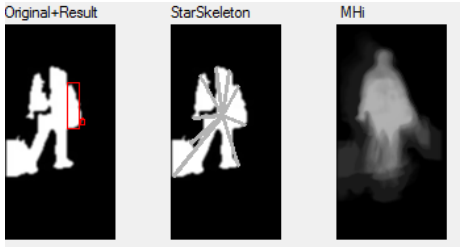 t3 Original+Result StarSkeleton MHi 	time series graph
Seq.24	t1 Original+Result StarSkeleton MHi 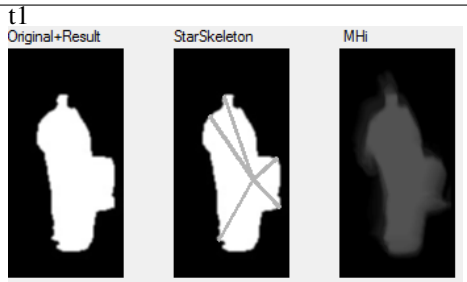 t2 Original+Result StarSkeleton MHi 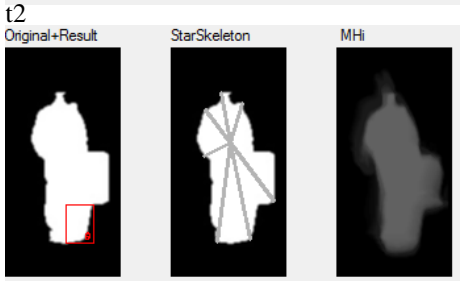 t3 Original+Result StarSkeleton MHi 	time series graph

Seq.25	t1 Original+Result StarSkeleton MHi t2 Original+Result StarSkeleton MHi t3 Original+Result StarSkeleton MHi 	time series graph
Seq.26	t1 Original+Result StarSkeleton MHi 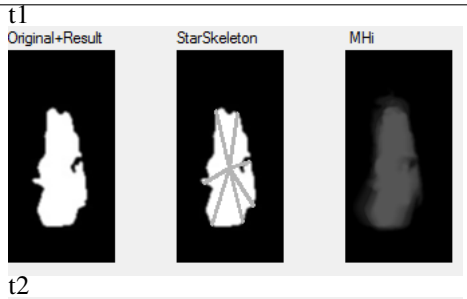 t2 Original+Result StarSkeleton MHi t3 Original+Result StarSkeleton MHi 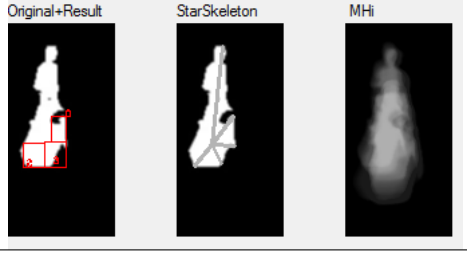	time series graph

Seq.27	t1 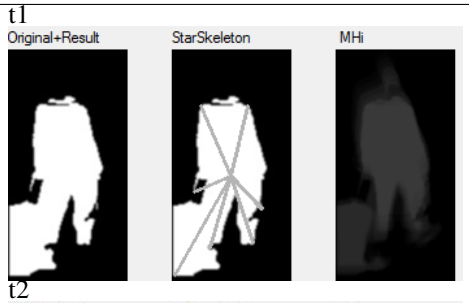 t2 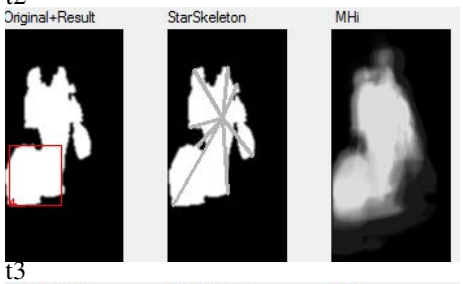 t3 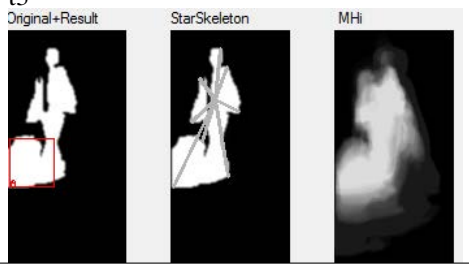	time series graph 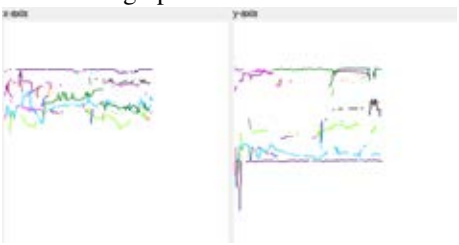
Seq.28	t1 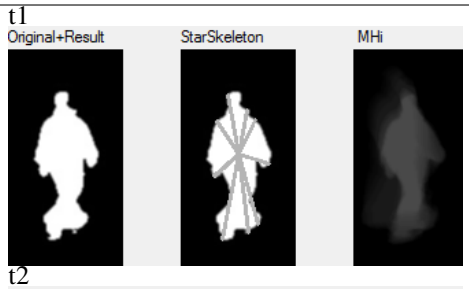 t2 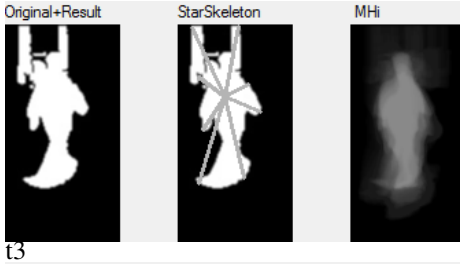 t3 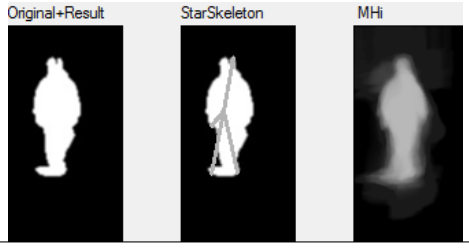	time series graph

Seq.29	t1 Original+Result StarSkeleton MHi 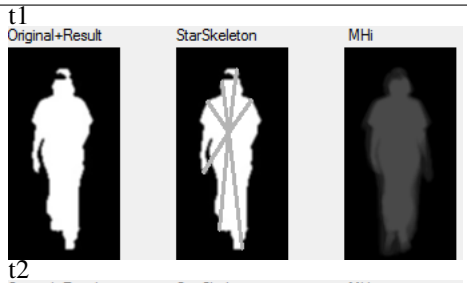 t2 Original+Result StarSkeleton MHi 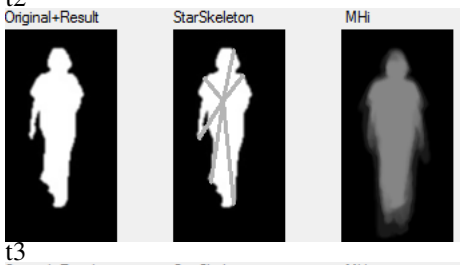 t3 Original+Result StarSkeleton MHi 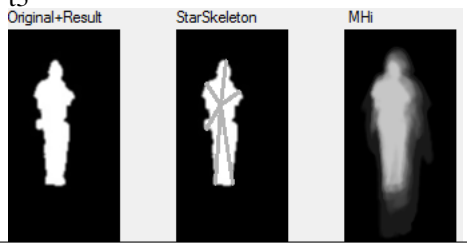	time series graph 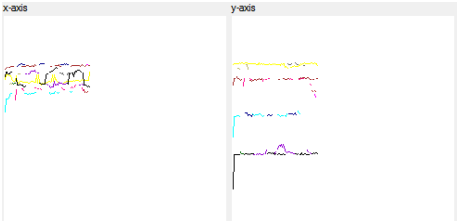
Seq.30	t1 Original+Result StarSkeleton MHi 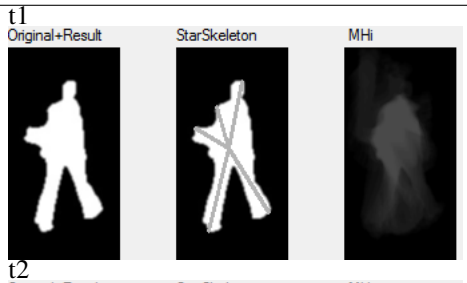 t2 Original+Result StarSkeleton MHi 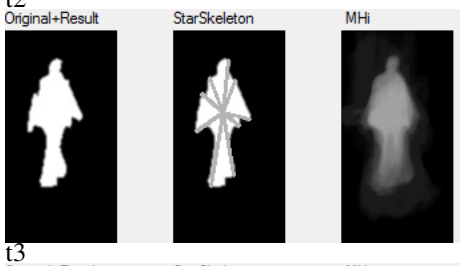 t3 Original+Result StarSkeleton MHi 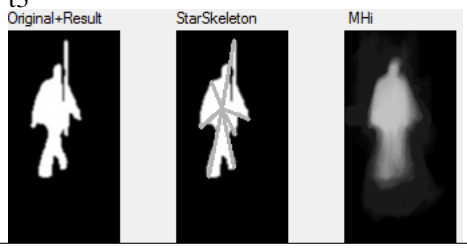	time series graph 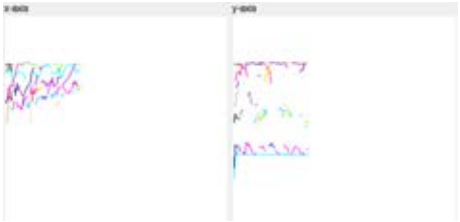

Seq.31	t1 Original+Result StarSkeleton MHi t2 Original+Result StarSkeleton MHi t3 Original+Result StarSkeleton MHi 	time series graph 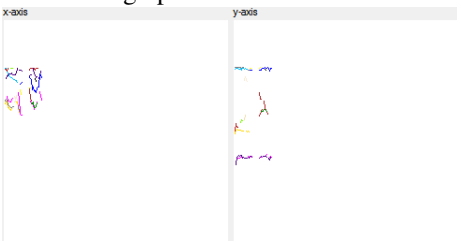
Seq.32	t1 Original+Result StarSkeleton MHi 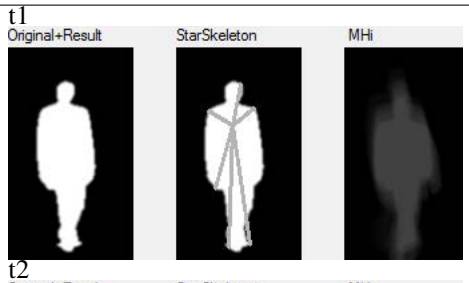 t2 Original+Result StarSkeleton MHi 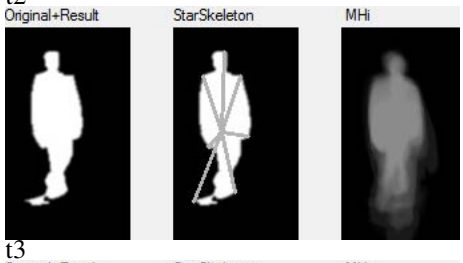 t3 Original+Result StarSkeleton MHi 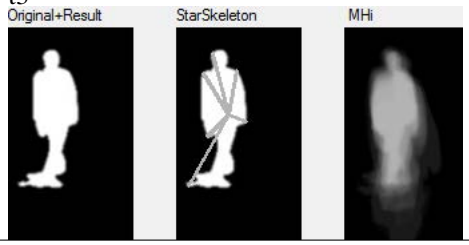	time series graph 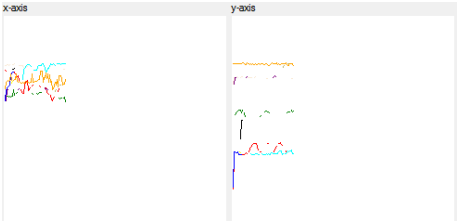

Seq.33	t1 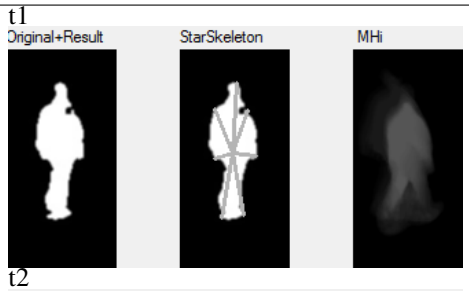 t2 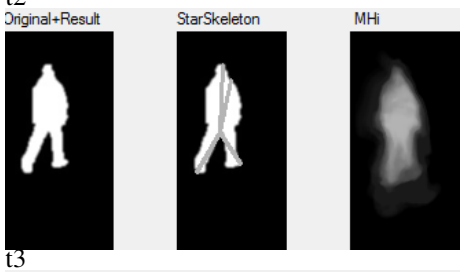 t3 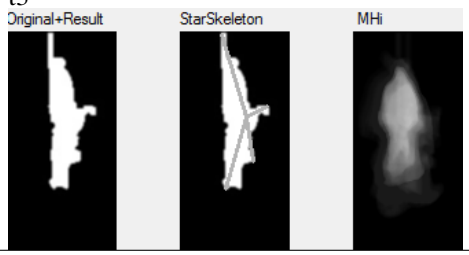	time series graph
Seq.34	t1 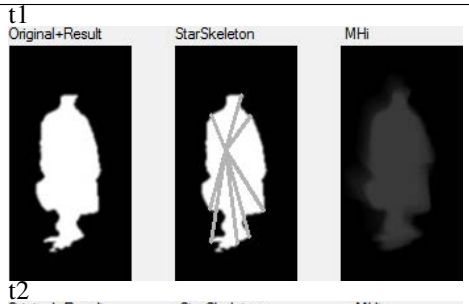 t2 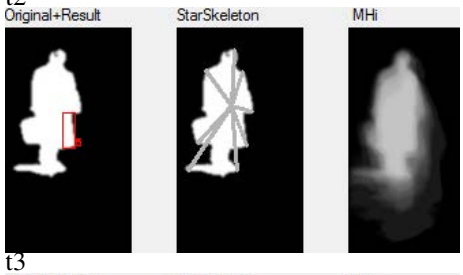 t3 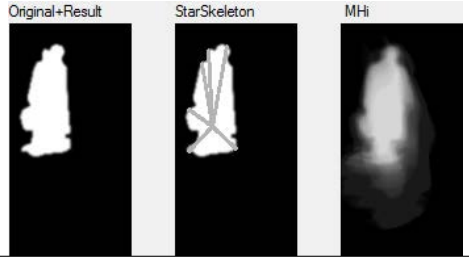	time series graph 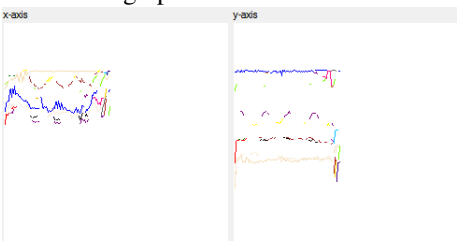

Seq.35	t1 Original+Result StarSkeleton MHi t2 Original+Result StarSkeleton MHi t3 Original+Result StarSkeleton MHi 	time series graph
Seq.36	t1 Original+Result StarSkeleton MHi t2 Original+Result StarSkeleton MHi t3 Original+Result StarSkeleton MHi 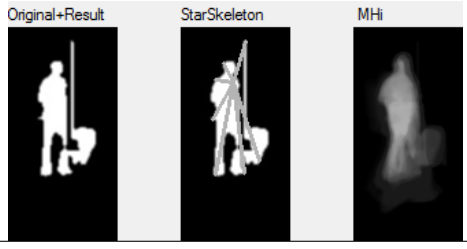	time series graph

Seq.37	t1 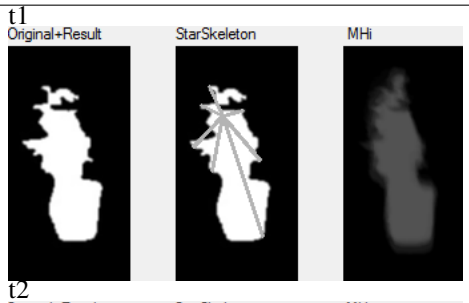 t2 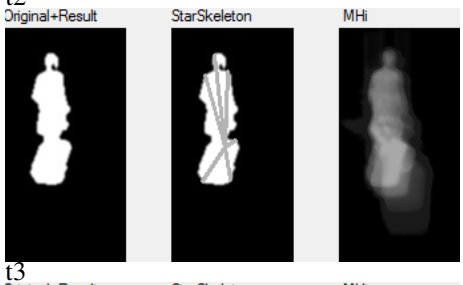 t3 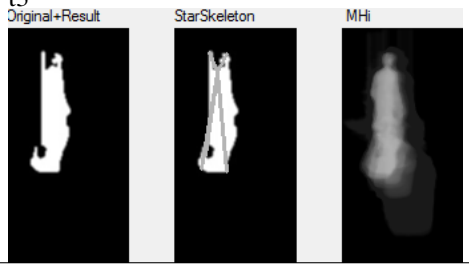	time series graph 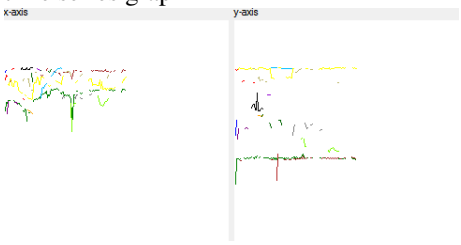
Seq.38	t1 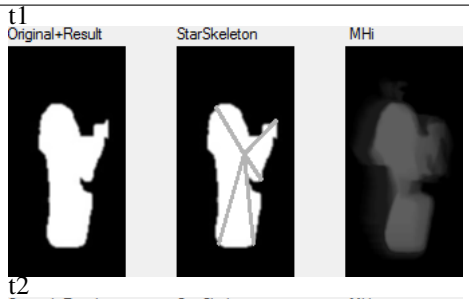 t2 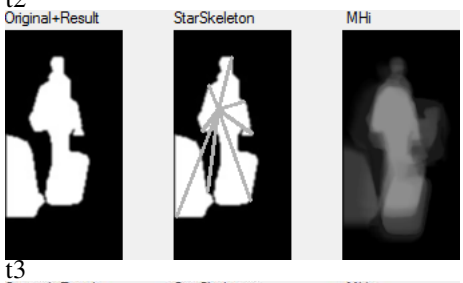 t3 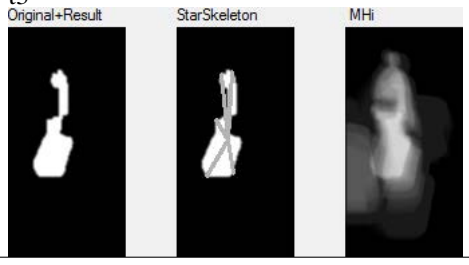	time series graph

Seq.39	t1 Original+Result StarSkeleton MHi t2 Original+Result StarSkeleton MHi t3 Original+Result StarSkeleton MHi 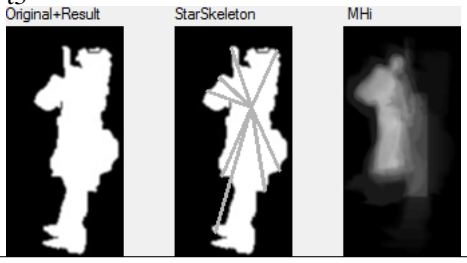	time series graph

Biography

Rawin Chayanurak received his B.Sc. in Information and Communication Technology from Mahidol University in 2009. Currently, she is pursuing her master degree in image and video processing on surveillance camera at Computer Science and Information Technology Program, Department of Mathematics and Computer Science, Faculty of Science, Chulalongkorn University.

International Conference Proceedings Rawin Chayanurak, Nagul Cooharojananone, Shinichi Satoh, and Rajalida Lipikorn, ”Carried Object Detection using Star Skeleton with Adaptive Centroid and Time Series Graph”, 10th International Conference on Signal Processing, pp. 736-739, Oct. 24-28, 2010. (ISBN: 978-1-4244-5897-4)